

Politecnico di Torino



Corso di Laurea Magistrale in Ingegneria Meccanica

Tesi di Laurea Magistrale

Study of injection strategies on a Diesel Engine:
Experimental evaluation of a split injection combustion
and proposal of a new combustion chamber design

Relatore: Prof. Alessandro Ferrari

Corelatore: Dott. Kazuki Inaba

Candidata: Lucia Del Bianco

A.A. 2018/2019

ACKNOWLEDGMENTS

First and foremost, I want to express my gratitude to Mr. Inaba, for the time he gifted me, patiently answering my questions and constantly supporting me during my permanence in the Engine System Laboratory of the Hokkaido University.

I would like to express my sincere thanks to Professor Ogawa, Professor Kobashi and Professor Shibata for accepting me in the laboratory, providing me a great chance of learning, and to Professor Ferrari, for entrusting me from the very start and for his valuable advice, which I needed to carry out this project miles away from Politecnico di Torino.

A warm thanks goes to the members of the laboratory, for enriching my everyday life experience in Japan, always making me feel like I belonged to the team, in spite of the language and culture barriers.

Throughout my master in Torino I met precious friends, which not only shared with me part of their student life, but also inspired me and shaped me as a person: I want to thank Najlae for showing me what persistence is and Davide for teaching me to believe in myself and the value of hard-work.

A special thanks goes to Ceci, for being with me during the neverending nights before exams, and to Shair for motivating me towards positivity despite troubles one can encounter. Thank you Hamid, Smriti, Das and the e^3 Hokudai group for living with me happy exploration moments in Hokkaido.

Last but not least, I strongly value the constant presence of my big family, to which I want to express my gratefulness for always providing me with the resources I needed to achieve my goals and, especially, for teaching me to think outside the box.

LDB

Contents

1	Introduction	1
1.1	Background	1
1.2	Purpose and methods	5
2	Literature review	6
2.1	Compression Ignition Engines	6
2.2	Combustion techniques in compression ignition engines	6
2.3	Flame Types	6
2.4	Typical Diesel Combustion and Rate Of Heat Release	7
2.5	Pollutants formation	10
2.6	Alternative Compression-Ignition Combustion Techniques	12
2.7	Dual mode concept	15
2.8	Semi-premixed diesel combustion	16
3	Experimental Apparatus	18
3.1	Hardware	18
3.2	Software	22
4	PART 1: Comparison of partially premixed diesel combustion and conventional diesel combustion	26
4.1	Experimental Procedure	26
4.1.1	Comparison between partially premixed and conventional diesel combustions	26
4.1.2	Influence of combustion phase	29
4.1.3	Influence of EGR ratio on partially premixed combustion	29
4.1.4	Computational investigation of combustion mechanism at low engine load	29
4.2	Results and Discussion	31
4.2.1	Comparison between partially premixed and conventional diesel combustions	31
4.2.2	Influence of combustion phase	36

4.2.3	Influence of EGR ratio on partially premixed combustion	40
4.2.4	Computational investigation of combustion mechanism at low engine load	41
5	PART 2: Enhanced air utilization through spray-dividing combustion chamber design	44
5.1	Overview of the divided combustion chamber concept aimed at an improved air utilization	44
5.1.1	Previous study on the divided combustion chamber concept	44
5.1.2	Current study on the divided combustion chamber concept	48
5.2	Experimental procedure	50
5.3	Results and discussion	52
6	Conclusions	55

List of Tables

1	<i>Engine specifications</i>	18
2	<i>JIS No. 3 Fuel Specifications</i>	19
3	<i>Nozzles' specifications</i>	20
4	<i>Experimental conditions</i>	28
5	<i>CA50 settings for the study of combustion phase</i>	29
6	<i>Sub-models in CFD code FIRE</i>	30
7	<i>Experimental conditions for the computational simulations of the Partially Pre-mixed Combustion</i>	50

List of Figures

1	<i>Globally averaged greenhouse gas concentrations [1]</i>	1
2	<i>Globally averaged combined land and ocean surface temperature anomaly [1]</i> . . .	1
3	<i>Emissions by share in the European Economic Area, 2018 [13]</i>	2
4	<i>Evolution of European norms on NO_x and PM emissions for passenger vehicles [8]</i>	3
5	<i>Evolution of European norms on NO_x and PM emissions for light commercial vehicles [8]</i>	3
6	<i>Rate of heat release over crank angle of a conventional diffusive diesel combustion</i>	9
7	<i>Model of the soot formation process in a typical diesel combustion flame [11]</i> . .	10
8	<i>Kamimoto map: soot and NO_x formation areas on a $\phi - T$ map</i>	11
9	<i>Kamimoto map with displayed conventional and alternative combustion strategies</i>	13
10	<i>Dual mode operation concept</i>	16
11	<i>(a) Premixed diesel combustion; (b) Partially premixed diesel combustion</i>	17
12	<i>Layout of experimental setup</i>	18
13	<i>Stepped-lip re-entrant combustion chamber with single injector</i>	20
14	<i>Divided combustion chamber with two injectors</i>	21
15	<i>Divided combustion chamber's spray's cone angles</i>	21
16	<i>Heat balance diagram</i>	23
17	<i>(a) Pilot-pilot-main Diesel Combustion; (b) Partially Premixed Diesel Combustion with triple fuel injection</i>	26
18	<i>Computational mesh of 1/10 sector of the Stepped-lip re-entrant combustion chamber</i>	30
19	<i>Comparison of pressure, temperature and Rate Of Heat Release versus Crank Angle among partially premixed combustion and conventional diesel combustion</i> .	32
20	<i>Heat balance and degree of constant volume of conventional and partially premixed diesel combustion at three engine loads</i>	33

21	<i>Maximum rate of pressure rise, combustion noise, NO_x and smoke emission levels of conventional and partially premixed diesel combustion at three engine loads</i>	35
22	<i>Pressure, temperature and ROHR plots for different combustion phases, at low and high loads, for Conventional Diesel Combustion and for Partially Premixed Diesel Combustion</i>	37
23	<i>Thermal efficiency related parameters evaluated at different combustion phases and engine loads for Conventional Diesel Combustion and Partially Premixed Diesel Combustion</i>	38
24	<i>Maximum rate of pressure rise, combustion noise, and NO_x and Particulate emissions obtained at different combustion phases, at low and high engine loads, for Conventional Diesel Combustion and for Partially Premixed Diesel Combustion</i>	39
25	<i>NO_x reduction by EGR, with effects on emissions and thermal efficiency, for Partially Premixed Diesel Combustion</i>	40
26	<i>Affidability of calculation results</i>	41
27	<i>Rate of cooling loss over the crank angle of the most advanced cases of Conventional and Partially Premixed combustions and of the most delayed case for Conventional combustion</i>	42
28	<i>Visualization of in-cylinder gas temperature and heat flux evolution at the combustion chamber's wall</i>	43
29	<i>Concepts of combustion in the standard Re-entrant combustion chamber (a), and combustions' spatial separation in a Divided combustion chamber (b)</i>	45
30	<i>Designs of Divided (a) and Re-entrant (b) combustion chambers</i>	46
31	<i>Rate of heat release in the Divided combustion chamber</i>	46
32	<i>NO_x and Particulate emissions and net indicated thermal efficiency as functions of the intake oxygen concentration, for the PPCI with the Divided and the Re-entrant combustion chambers</i>	47

33	<i>Concept of divided combustion chamber where injection angle is: (a) fixed and narrow, (b) fixed and wide, or (c) variable</i>	49
34	<i>New Divided combustion chamber design and double injector system</i>	49
35	<i>Computational mesh of the Stepped-lip re-entrant combustion chamber</i>	51
36	<i>Computational mesh of the new Divided combustion chamber</i>	52
37	<i>Rate of heat release in new Divided and Stepped-lip re-entrant combustion chamber</i>	52
38	<i>Temperature and O₂ distributions of in-cylinder gasses over the crank angle period from 2 to 8 °CA ATDC.</i>	53

List of Abbreviations

AR5	Fifth Assessment Report on Climate of 2014
ATDC	After top dead centre
BEV	Battery electric vehicles
BTDC	Before top dead centre
CA	Crank angle
CI	Compression ignition
CLD	Chemical luminescence detector
CN	Combustion noise
COP21	21 st Conference of the Parties (to the 1992 United Nations Framework Convention on Climate Change)
CPL	In-Cylinder Pressure Level
DI	Direct injection
DOC	Diesel oxidation catalyst
DPF	Diesel particulate filter
EEA	European Environmental Agency
EGR	Exhaust Gas Recirculation
EU	European Union
EVO	Exhaust valve opening
FCEV	Fuel cell electric vehicles
FID	Flame ion detector
HCCI	Homogeneous charge compression ignition
IMEP	Indicated Mean Effective Pressure
IPCC	Intergovernmental Panel on Climate Change
ICE	Internal combustion engine
IVC	Intake valve closing
LTC	Low temperature combustion
NDIR	Non-dispersive infrared sensor
PCCI	Premixed charge compression ignition
PCI	Premixed charge compression ignition
PM	Particulate Matter
PPCI	Partially premixed compression ignition
ROHR	Rate of heat release
SA	Structure Attenuation
SCR	Selective reduction catalyst
SI	Spark ignition
THC	Total hydrocarbons
WHO	World Health Organization

Summary

The present work's goal is to experimentally define the advantages in terms of NO_x and Particulate emissions and thermal efficiency of a split injection, namely an unconventional combustion strategy implemented on a diesel engine, here called Partially Premixed Diesel Combustion (PPCI).

The hardware of the experimental setup consists of a single-cylinder, four-stroke, supercharged, direct injection, diesel engine. The software utilized for the computational simulations of the combustion process is AVL Fire, while engine-out data is reprocessed with the help of an Excel code based on the heat balance equation.

Initially, a comparison of the Partially Premixed Diesel Combustion with the Conventional Diesel Combustion is carried out at three different engine loads (low, medium and high). A pilot-pilot-main injection strategy is selected for the Conventional Diesel Combustion. A triple injection is implemented for the Partially Premixed Diesel Combustion, resulting in a two-stage heat release: the first one typically produced by a premixed-like flame, the second one by a diffusion flame. Thermal efficiency, noise and emissions are monitored along with the change of the combustion phase and with the implementation of Exhaust Gas Recirculation. Finally, simulations are run on a new proposed combustion chamber design which is coupled with a double-injector system and has the goal of spatially separate the premixed flame and the diffusion flame, promoting a better in-cylinder air utilization.

Improvements in terms of emissions and thermal efficiency are generally achieved by the PPCI only at low and medium loads, while noise levels remain comparable with the conventional case at high load and slightly increase at low and medium loads. Simulations on the new combustion chamber suggest that an air utilization improvement locally takes place.

1 Introduction

1.1 Background

In recent decades, the impact on natural and human systems caused by change in climate have been observed all over the world, as reported by IPCC (Intergovernmental Panel on Climate Change) in the Fifth Assessment Report (AR5) on climate of 2014 [1]. The land and ocean combined surface temperature showed a warming of $0.85\text{ }^{\circ}\text{C}$ over the period 1880 to 2012 and the anthropogenic greenhouse emissions' trend (Figure 1), which has been positive since the pre-industrial, is extremely likely to be the dominant cause of the observed warming since the mid-20th century (Figure 2).

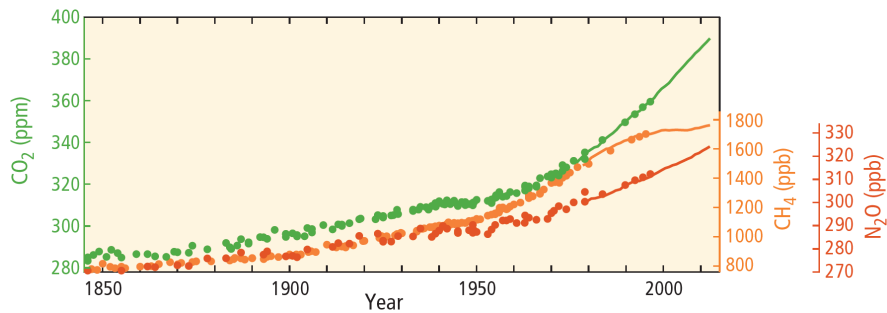


Figure 1: Globally averaged greenhouse gas concentrations [1]

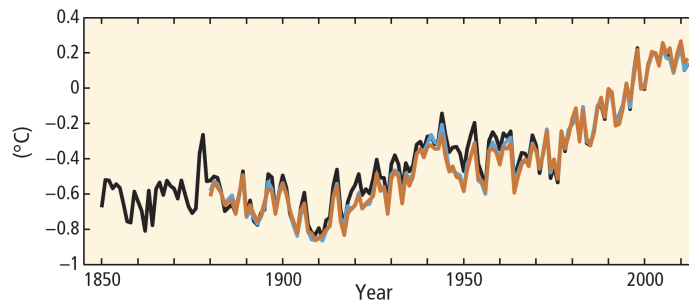


Figure 2: Globally averaged combined land and ocean surface temperature anomaly [1]

Air pollution caused by anthropogenic emissions is also a serious threat to human health [2]. Air quality has been at critical levels, far above the World Health Organization's (WHO)

guidelines, for several years, affecting economies and people’s quality of life. According to WHO’s document, 92 % of the world population is exposed to $PM_{2.5}$ air pollution concentrations that are above the annual mean [2].

Greenhouse gases (CO_2 equivalent) and main air pollutants generated in 2017 were differentiated by source by the European Environment Agency (EEA):

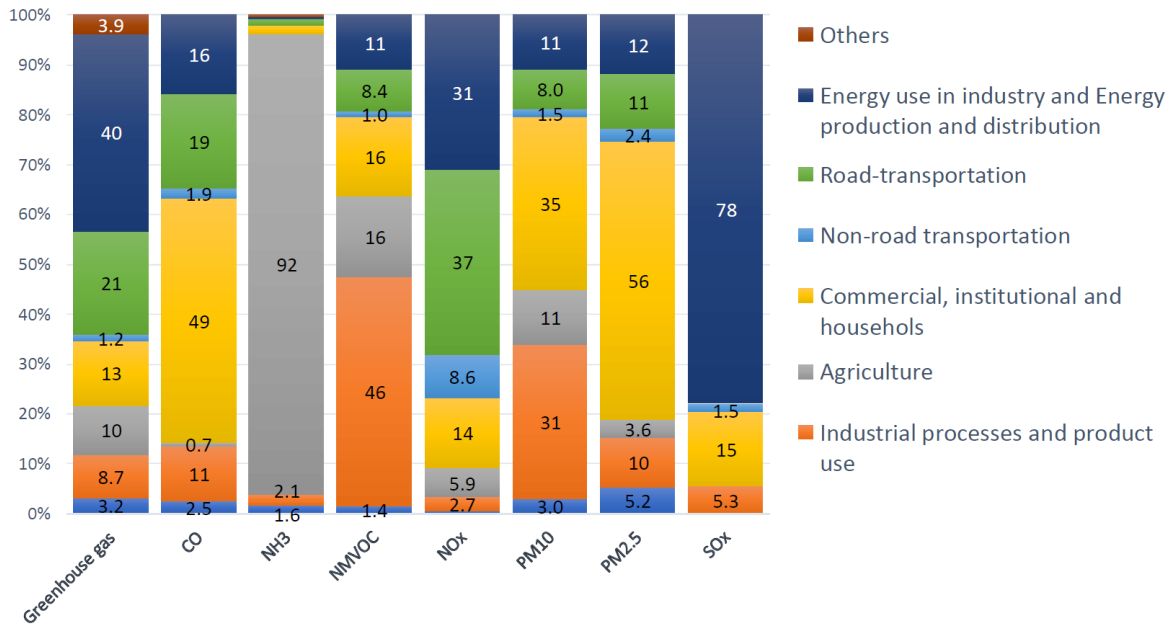


Figure 3: Emissions by share in the European Economic Area, 2018 [13]

According to EEA, road-transportation was responsible for 21% of the greenhouse gas emissions, 37% of NO_x emissions and 8% and 11% respectively of PM_{10} and $PM_{2.5}$ emissions in Europe.

In 2015, the Paris Convention was adopted at the United Nations Climate Change Conference (COP 21), stating the goal to keep the average global temperature rise well below $2^\circ C$ from before the industrial revolution values [3]. In response to this, the measures adopted by the EU on the sector of transportation resulted on year by year increasingly stringent norms on vehicles’ emission (Figures 5 and 4).

Recently, focus has been put on next-generation vehicles, such as battery electric vehicles (BEV) and fuel cell vehicles (FCEV), due to the rising awareness of global warming and envi-

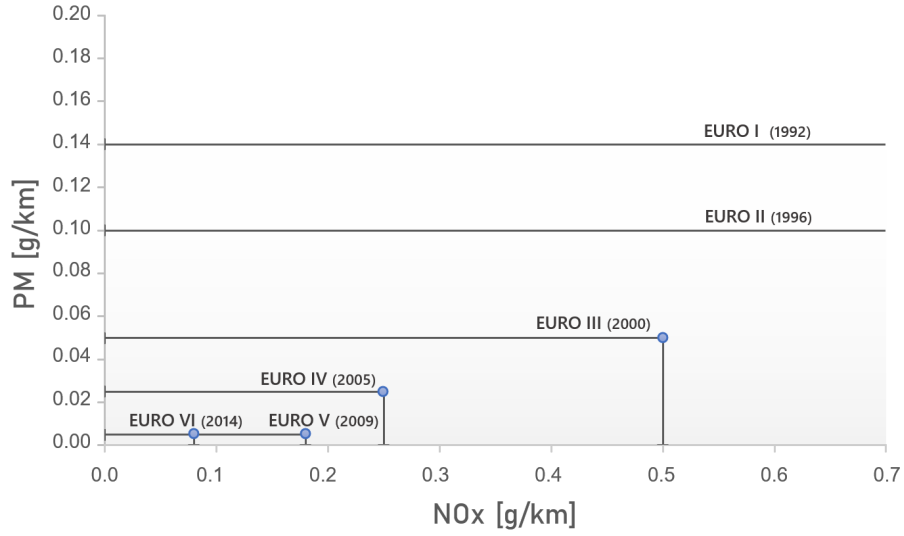


Figure 4: Evolution of European norms on NO_x and PM emissions for passenger vehicles [8]

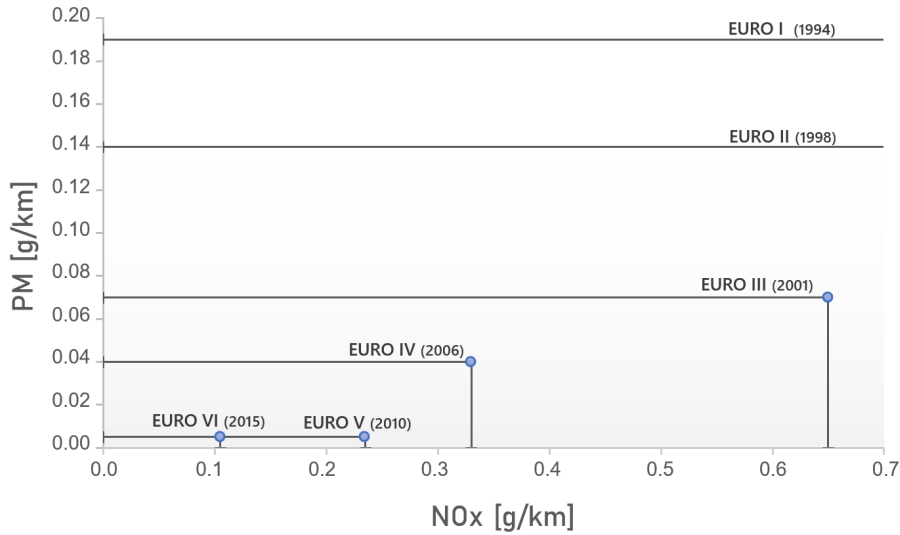


Figure 5: Evolution of European norms on NO_x and PM emissions for light commercial vehicles [8]

ronmental problems [7].

However, according to the EEA, their current diffusion in the European Union is still limited (in 2017 electric vehicles accounted only for 1.5% of new car registrations) and their sales are expected to increase at a slow pace in the next decades. Moreover, a proper evaluation through a Life Cycle Assessment (LCA), shows that the emissions and the negative impact on the environment, related to their implementation, would be non-negligible. Furthermore, at

present, large vehicles, heavy duty vehicles and ships are mostly powered by diesel engines, and their complete electrification seems extremely unrealistic, since no other effective alternative has been found yet.

The two main types of ICE on the market are spark ignition (gasoline) and compression ignition (diesel) engines, which shared respectively 52.6 % and 44.5 % of the market of new passengers cars in Europe in 2017 [9]. Since diesel engines are not limited by spark knock, higher compression ratios and higher supercharging can be realized with respect to gasoline engines. The engine load is controlled by the amount of fuel injected directly in the combustion chamber, producing smaller pumping losses. Thermal efficiency results to be higher than that of gasoline engines [10].

Despite their high thermal efficiency, the weak point of diesel engines is the difficulty in the reduction of harmful components in the exhaust gas. The main harmful substances produced and emitted from internal combustion engines are carbon monoxide (CO), unburned hydrocarbons (HC), nitrogen oxides (NO_x) and particulate matter (PM). The concentrations of NO_x from diesels are comparable with those of gasoline engines, but they are a major source of particulate emissions [10].

To meet the European Emission Standards on emissions of the just cited air pollutants by diesel (and gasoline) engines, over the years, manufacturers have improved engine combustion and developed various exhaust after-treatment technologies. These include Diesel Particulate Filter (DPF) for the reduction of PM, Selective Reduction Catalyst (SRC) for the reduction of NO_x and Diesel Oxidation Catalyst (DOC) to purify exhaust from CO and THC [4].

However, exhaust post-treatment systems used for diesel engines are complicated compared to gasoline engines, which can use the cheaper and with high purification rate three-way catalysts [5].

The above considerations explain the effort that, at the present moment, in research, is being done to achieve emissions reduction by combustion efficiency improvement in diesel engines.

1.2 Purpose and methods

The current research's aim is to investigate ways of improving the emissions performance of a diesel engine, with particular focus on NO_x and particulate matter, while maintaining its high thermal efficiency.

The analysis and comparison of the semi-premixed or partially premixed combustion with the conventional diesel combustion are carried out in the first part of the project. For this purpose, a single-cylinder four-stroke diesel engine is utilized as well as a 3D combustion simulation software. The effect of combustion phase over different load conditions is investigated by varying the fuel injection timings, pressure and amount per injection.

In the second part of the research a new combustion chamber design, injection system and injection strategy is proposed. It is a concept studied for the implementation of the semi-premixed combustion. Starting from considerations on a previous design, the new model is developed and simulations are carried out by means of the 3D combustion simulation software.

2 Literature review

2.1 Compression Ignition Engines

In compression ignition engines, commonly referred to as diesel engines, during the intake stroke air enters the cylinder alone while fuel is injected later, at high pressure (with modern common rail systems the typical range is between 1000 to 2000 bar, or higher), directly in the cylinder. Due to the absence of the knocking limit which is found in gasoline engines, the compression ratio of diesel engines can be higher (typically in the range 14 to 22), resulting in a relative improvement of the efficiency in terms of fuel conversion. Another factor influencing positively the efficiency of the diesel engine is the absence of pumping loss which in gasoline engines is typically induced by the throttle valve at the intake. Load is controlled by fuel quantity injected per cycle, while air quantity remains constant and can be aspirated at atmospheric pressure, or pre-compressed through turbocharging or supercharging. These two latter techniques are commercially implemented to achieve a certain power output with engines resulting smaller in size and thus lighter [10].

2.2 Combustion techniques in compression ignition engines

Combustion, in compression ignition engines, occurs after the fuel is injected in the combustion chamber and gets in contact with the high temperature and high pressure compressed gaseous mixture (air and eventually exhaust gas from Exhaust Gas Recirculation system). It is overall a complex mechanism due to the numerous processes and variables involved: fuel atomization, evaporation, air entrainment, ignition and combustion itself. It is an unsteady process that varies strongly with engine's operating conditions, and which involves turbulent flames [10].

2.3 Flame Types

Flame, by definition, is the zone where the combustion process occurs, and can be classified in premixed flames and diffusion flames by the state or condition of mixedness of fuel and

oxidizer [14]. In premixed flames, reactants are mixed at the molecular level before the start of the oxidizing process, while, in diffusion flames, the reactants are not uniformly mixed and the oxidizing reaction occurs only at the interface of the two, where the mixing by molecular diffusion takes place.

2.4 Typical Diesel Combustion and Rate Of Heat Release

In production diesel engines, typically, the injection strategy consists of a single injection of fuel which ignites after a short ignition delay (about 5° CA). The energy is released by the fuel initially through a short premixed flame phase, and then, by the great part, during the subsequent mixing-controlled or diffusion flame.

The simplicity of implementation and the relatively high thermal efficiency [17] of this strategy made it the most used strategy in nowadays (and ever) compression-ignition combustion engines.

An important instrument for the analysis of the combustion processes, which will also be used extensively in this paper to describe the different combustion strategies and to comment the experimental results, is the Rate Of Heat Release (ROHR), namely the rate at which the burning fuel, releases its chemical energy. Heywood, in Internal Combustion Engine Fundamentals [10], presents a simplified method to obtain the ROHR from the measured data of pressure versus crank angle, starting from the first law of thermodynamics for an open system:

$$\frac{dQ}{dt} - p \frac{dV}{dt} + \sum \dot{m}_f \cdot h_f = \frac{dU}{dt} \quad (1)$$

where:

$\frac{dQ}{dt}$: rate of heat transfer into the system across the system boundary [W];

$p \frac{dV}{dt}$: rate of work done by the system on the piston, with the system's boundary displacement [W];

\dot{m}_f : injected fuel mass flow (crevices mass flow is neglected for simplicity) [kg/s];

h_f : enthalpy of the injected fuel [J/kg];

U : internal energy of the content of the cylinder [J];

Energy and enthalpy are considered as the sensible energy ($U = U_s$) and sensible enthalpy ($h = h_s$). Namely the physical quantities decumulated from the heat of formation. The rate of heat transfer, in this case, results to be the difference between the rate of chemical energy released by the fuel and the rate of heat transferred from the system to the environment $(dQ)/dt = (dQ_n)/dt = (dQ_{chemical})/dt - (dQ_{heattransfer})/dt$. Since the sensible enthalpy of fuel is close to zero, the term can be neglected. Moreover, in this case the system is approximated as homogeneous, which is far from the real process, and the contents of the cylinder are modelled as ideal gasses.

Through these simplifications, the net rate of heat release can be written as:

$$\frac{dQ_n}{dt} = \frac{\gamma}{\gamma - 1} p \frac{dV}{dt} + \frac{1}{\gamma - 1} V \frac{dp}{dt} \quad (2)$$

where:

γ : ratio of specific heats, c_p/c_v ;

In this research, the ROHR of combustions in real engine tests was obtained as the summation of net heat release rate (calculated, by an Excel code, in a similar way to that just explained) and the rate of heat transfer to the cylinder walls, calculated by the one dimensional Woschni's equation, modelling convective heat transfer.

The following Figure 6 shows the ROHR over the crank angle of a typical diesel combustion.

The ignition delay interval goes from the injection start moment to the ignition point. Its duration, which is kept relatively short in this case (from -1.5°CA ATDC to 2.5°CA ATDC), has, in general, a strong influence on the magnitude of the initial peak of heat release increase rate [10], which corresponds to the premixed combustion phase (2.5°CA ATDC to 5°CA ATDC). Such type of combustion is possible thanks to the time that the fuel gets to evaporate during

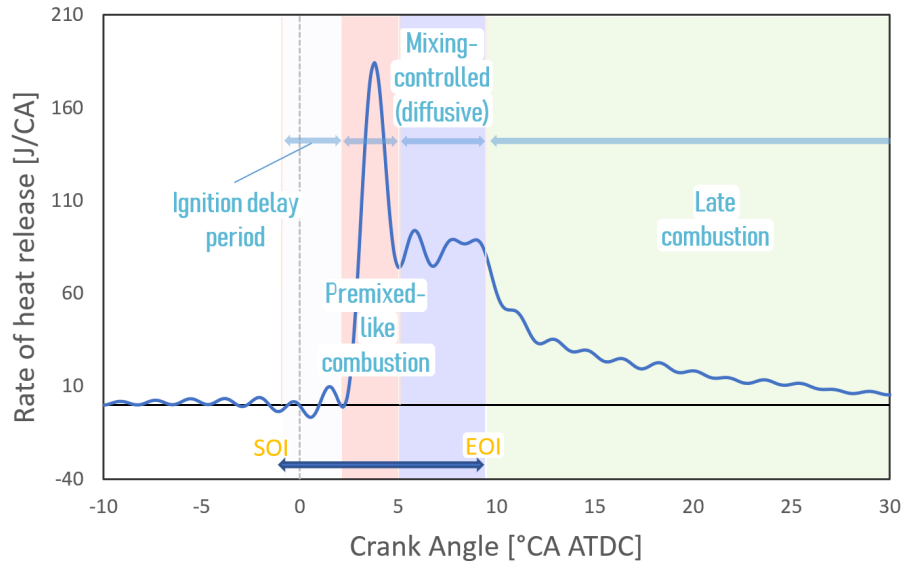


Figure 6: Rate of heat release over crank angle of a conventional diffusive diesel combustion

the delay period and to mix with in-cylinder gas. In the graph, the period between the ignition point to the end point of premixed combustion is denominated "Premixed-like combustion": in a diesel engine, combustion is not perfectly premixed, since the homogeneity of the air-fuel mixture is not high, as, for example, in a gasoline engine.

The mixing-controlled phase follows, resulting in the second peak on the ROHR graph, with milder gradients. This stage occurs from just after the premixed phase to the injection end point and it is followed by a late combustion phase during which the lowering temperature and pressure of the expansion stroke contribute to the decrease of the rate of heat release.

The balance between the premixed and the mixing-controlled stage of combustion is the key for the control of the engine-out emissions such as NO_x and particulate matter. For this reason, in the years, a variety of optical techniques has been used to investigate the local evolution process of combustion flames.

2.5 Pollutants formation

In this paragraph the PM and NO_x generation mechanisms is briefly discussed.

In Figure 7 it is presented a model of typical diesel spray flame development, based on the optical study of Kosaka et al. [11]. In this analysis focus is put on the processes of ignition, formation of soot precursors and soot itself, and soot oxidation by OH .

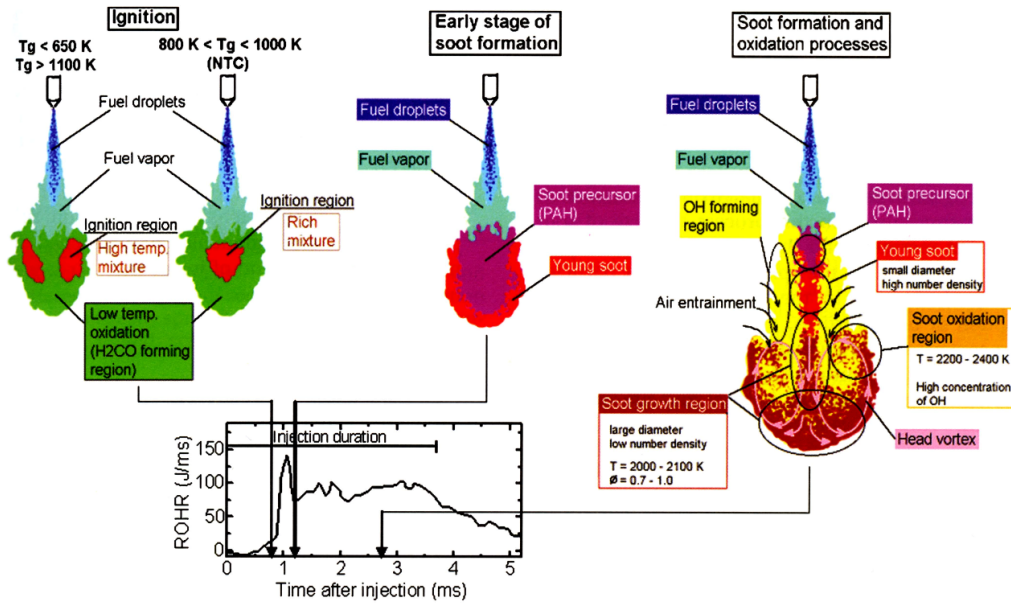


Figure 7: Model of the soot formation process in a typical diesel combustion flame [11]

As can be seen from the figure, at the ignition stage, low temperature oxidation of fuel happens, with the appearance of H_2CO (formaldehyde) (green zone). Hot ignition then takes place (red zone) at the periphery or at the central region and H_2CO is quickly consumed. The following stage is the short early soot formation phase: soot precursors, PHA (polycyclic aromatic hydrocarbons), appear in the leading region of the fuel spray flame, while young soot forms at its periphery. The third and longer stage of heat release, which takes place as the mixing-controlled flame is established, is represented on the right. Soot precursor are generated in the central part of this turbulent diffusion flame, young soot forms just downstream and grows in size while decreasing in number of particles as it moves towards the flame tip. Head

vortexes push the soot particles on the periphery of the spray, from where they move upstream by convection, entering the fuel-lean burning mixture at the sides of the flame. Here, the OH radicals generated from the high temperature field oxidize most of the soot.

Kosaka et al. study focused on tracking the OH radicals as main soot oxidizers at high temperatures, but there are various other species which can serve the same purpose: O , O_2 , OH and H_2O . The balance between the formation and the burnout processes rules the soot engine-out emissions [10].

The oxidation of molecular nitrogen (N_2) at high temperatures and equivalence ratios close to stoichiometric, results in the production of NO and NO_2 (together addressed to as NO_x), where the latter typically accounts for about 10 % to 30 % of the total nitrogen oxides produced. Nitrogen oxides formation occurs in the high temperature ($T \geq 2000K$) and low fuel-air equivalence ratio (ϕ up to 1.1) zones [10], which are the same conditions at which OH radicals form and soot oxidation takes place. This is known as the soot- NO_x trade-off relationship, because of which the two components cannot be reduced contemporary using only the conventional strategy [17]. The typical NO_x and soot formation conditions in diesel engines, previously discussed in the paragraph, can be displayed in a ϕ - T map like the following, also known as the Kamimoto map [10]:

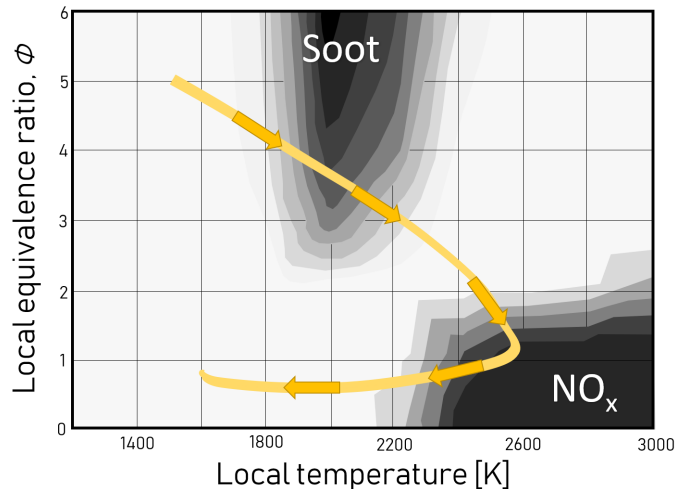


Figure 8: Kamimoto map: soot and NO_x formation areas on a $\phi - T$ map

The in-cylinder dynamically changing conditions achieved during the typical diesel combustion are here indicated by the yellow line. It must be noted that temperature and equivalence ratio are highly non-homogeneous inside the cylinder during the combustion process, therefore the evolution of in-cylinder gas-fuel mixture are represented with a certain degree of approximation.

To achieve a reduction of both types of emissions by performing a combustion which avoids the respective pollutant generation regions on the $\phi - T$ map, and to solve the issue of high combustion noise of the conventional diesel combustion, different combustion techniques have been investigated during the last few decades and will be shortly presented in the following paragraphs.

2.6 Alternative Compression-Ignition Combustion Techniques

A first option is to maintain diesel combustion as the main fuel energy release process, while adding smaller injections prior to or after the main one, with various purposes. This injection strategy can be easily implemented with the modern common rail technology [16].

Early pilot injection, typically accounting for about 5 to 15 % of the overall fuel quantity injected [10], can be implemented to shorten the ignition delay and therefore reduce the CN [15]. The main flame temperature generally decreases, eventually discouraging the generation of NO_x . Soot levels, on the other hand, typically increase since the reduced oxygen concentration before the main combustion and the shorter premixing time lead to higher equivalence ratios [15]. Because ignition delay is inherently shorter at higher loads, pilot injection has the biggest impact at low loads [10].

Post injection can be implemented with a main benefit on emissions. With a proper timing, post injection has the potential to oxidize a fraction of the unburned fuel and to decrease the CO , HC and PM engine-out. Late post injections can also be exploited to raise the temperature of the exhaust gas entering the after treatment devices such as the DOC, improving in this way their efficiency [16].

Some of the advanced or non-conventional strategies, which are based on enhancing the air/fuel mixing and/or highly diluting the O_2 in the intake gas through high EGR rates, are Homogeneous Charge Compression Ignition (HCCI), Low Temperature Combustion (LTC), Premixed Charge Compression Ignition (PCCI or PCI), and others [20] (Figure 9).

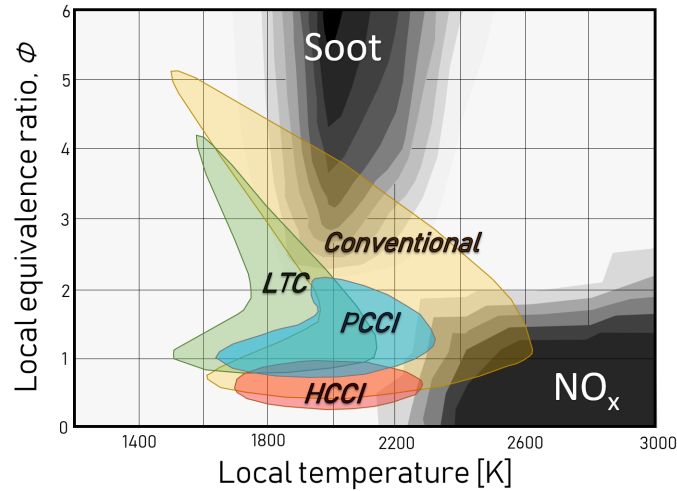


Figure 9: Kamimoto map with displayed conventional and alternative combustion strategies

In HCCI the characteristics of the two most popular internal combustion engine types are merged: the air-fuel mixture is homogeneously distributed prior to ignition, as it is for SI engines, while the actual start of combustion is not controlled by a spark plug but by the autoignition of the mixture itself as in CI engines. To achieve such a lean and homogeneous mixture prior to combustion, both Indirect Injection (mixing of fuel and air outside of the cylinder) or Direct Injection (mixing occurs inside the cylinder) can be used [17]. In the case of DI the fuel must be introduced early (up to 70° or 80° BTDC), to get enough time to completely evaporate and to produce a well-mixed lean charge. The resulting ROHR profile is smooth since the premixed and diffusion stages of the conventional diesel engine are not any more distinguishable: the combustion is only premixed [10]. Thanks to its lean mixture, the main advantage of the HCCI is to avoid the regions of the $\phi - T$ map where soot and NO_x usually form (see Figure 9). Moreover, the degree of constant volume (the ratio of theoretical work obtained from heat at each crank angle and the theoretical work of the Otto cycle working

over the engine’s compression ratio) is increased, with consequent benefits on efficiency [17]. The weak point of this strategy is the limitation of its application at low loads. In fact, at higher loads, a too much steep pressure rise resulting from the premixed combustion would cause unacceptable noise and even engine damage, and the higher flame temperatures would lead to an increase in NO_x production [17].

LTC strategy is based on the great reduction of combustion temperature by the implementation of large rates of EGR. It is also called “smokeless rich diesel combustion” [19] since, by extremely decreasing the oxygen content (to concentrations below 12 %), the *soot*– NO_x trade-off disappears: soot decreases to barely zero while NO_x remains ultra-low [21]. As it is possible to see from Figure 9, the low temperature enables the suppression of soot emissions even with high equivalence ratios. Even if rich mixture condition does occur, the PAH cannot react to form soot in such low temperature conditions [19]. From Figure 9, it is possible to evince the clear difference between HCCI and LTC as they occupy different regions of the ϕ – T map: while the homogeneity of the mixture is fundamental for HCCI, in LTC no improvement in the mixture formation is needed but still smokeless combustion is achieved [19]. However, with regards to LTC, it must be pointed out that at very low-oxygen concentrations, while the Insoluble Fraction of PM (ISF or *dry soot*) is reduced significantly, the Soluble Organic Fraction (SOF) increases [21].

Rather than aiming at homogeneity by prolonging the ignition delay, as in HCCI, with PCI and other techniques focus shifts on increasing the mixing rates between air and fuel (degree of turbulence). In PCI the fuel injection should be completed before the start of ignition [18]. To accelerate the air-fuel mixing, high fuel injection pressure is very effective. To obtain a leaner mixture and/or to extend the ignition delay, EGR can be used at some extent. Shimazaki et al. studies show how NO_x and smoke emissions can be generally reduced with the implementation of an optimized PCI combustion, while HC and CO emissions’ and fuel economy’s levels remain comparable to conventional diesel combustion’s ones [18].

Advanced combustion strategies however, are generally applicable with good results only at low or medium loads. Under high load condition, PCI is subjected to diesel knocking [18] in a similar way to HCCI, as previously stated. In LTC, the higher fuel quantity with a strong EGR ratio causes a drop in thermal efficiency and a worsening of *CO* and THC emissions, even if smokeless combustion is achieved [21]. When, in order to suppress these emissions, higher oxygen content is enforced, for example by supercharging, higher temperatures cause soot formation, and steeper pressure rise translates in unacceptable engine noise.

2.7 Dual mode concept

On the basis of the just stated issues, the concept of dual mode operation has been proposed [18]. Based on this idea, depending on the load condition, operation can be switched between conventional diesel combustion and PCI, on the same conventional diesel engine and injection system. PCI would be implemented at low loads, where the after-treatment devices are not active due to the low exhaust gas temperature, while conventional diesel combustion would be enforced at high loads, where higher emissions can be efficiently managed by the after-treatment devices, which are active thanks to the high exhaust temperatures (Figure 10).

However, there are some challenges related to the actual implementation of the a dual-mode concept. First of all, there is an intrinsic difficulty in obtaining a robust and repeatable engine behaviour with PCI strategy. In fact, PCI exhibits high sensibility to small EGR ratio's fluctuations, to small injection settings variations and even to the type of fuel which is used (due to the fact that commercially available fuels have different cetane numbers). In actual engine operation, speed and load vary almost continuously, and so do combustion parameters (gas temperature, pressures and exhaust composition, etc.). Secondly, switchover between conventional and PCI modes would add additional variability to the already unstable engine parameters. A complex control technology which is able to monitor on a real-time basis the engine conditions

is necessary in order to make this concept fully functional and commercially feasible [18].

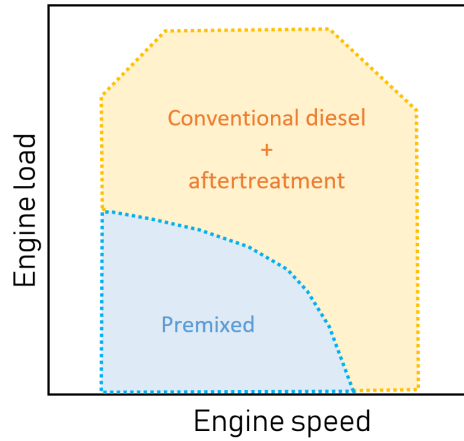


Figure 10: *Dual mode operation concept*

2.8 Semi-premixed diesel combustion

The concept of heat release splitting by separating the total fuel amount per cycle in two or more main injections is introduced in the here called “Partially Premixed diesel Combustion” or “Partially Premixed Compression Ignition” strategy (PPCI). This method is promising particularly for the reduction of noise which is obtained since the fuel chemical energy, released in two (or more) stages, produces lower peaking values than the ones of a single injection premixed strategy (Figure 11). In PPCI, depending on the injections’ timings, the two heat release stages might both exhibit premixed flame characteristics or show premixed behaviour for the first one and diffusive behaviour for the second one [20].

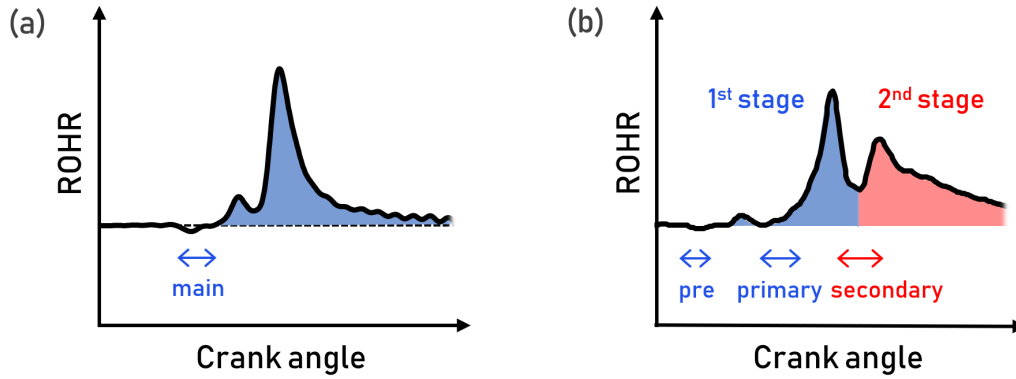


Figure 11: (a) *Premixed diesel combustion*; (b) *Partially premixed diesel combustion*

Recently, many studies have been carried out on the two-stage combustion, where the second peak suppresses the first peak rapid premixed combustion [22]. Ogawa et al. investigated the two-stage combustion, and indicated the twin peak shape of the heat release to be a good strategy to obtain, at medium load, high thermal efficiency, relatively low combustion noise, overall contained NO_x emissions, with unchanged levels of OH, THC and smoke, compared with the single stage premixed diesel combustion. Semi-premixed combustion's potential is its extension to a wider load range, namely the possibility to cover also medium and high loads (which is not feasible for the advanced combustion techniques previously described), eliminating the need for a complex dual-mode operating engine.

3 Experimental Apparatus

3.1 Hardware

The system consists of a single-cylinder, four-stroke, supercharged, direct injection diesel engine. The engine, mounted on a test bench, is connected to a start-up motoring system and water friction brake system. The cylinder has two intake and two exhaust valves. Other engine's specifications are summarized in Table 1, while the layout of the experimental setup is depicted in Figure 12.

Engine type	DI, single cylinder	
Displacement	550 cm ³	
Compression ratio	16.3	
	Stepped-lip re-entrant	Divided
Bore and stroke	ϕ85, 96.9mm	
Injection system	single	double
EGR system	Low pressure, intercooled	

Table 1: Engine specifications

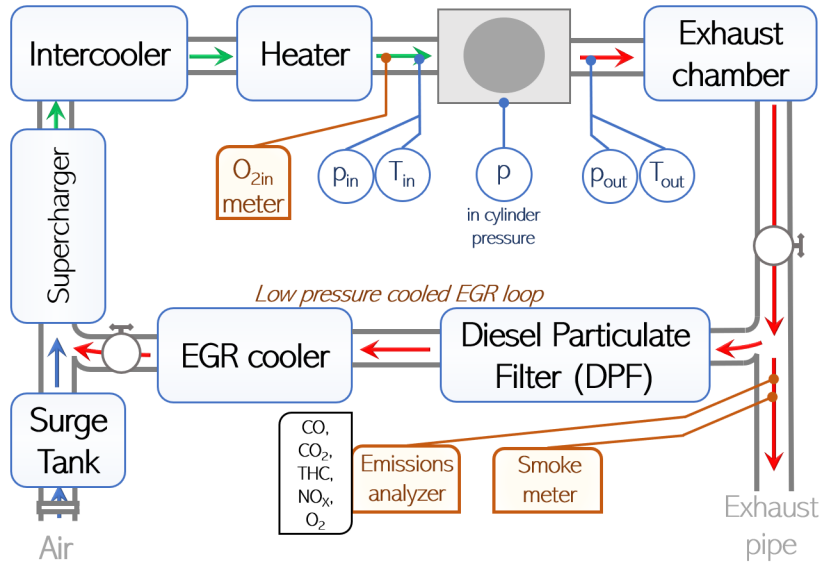


Figure 12: Layout of experimental setup

Gas pressure was measured by a piezo sensor (KISTLER S 103 A054-130) just before the intake port, by a piezo sensor (KISTLER 6052C) inside the cylinder and by a Bourdon tube

pressure gauge just after the exhaust port. Intake gas pressure p_{in} was always set at 120 *kPa* (*absolute*), by means of an electric motor driven supercharger, while the exhaust pressure p_{out} was always maintained equal to the intake pressure, utilizing a throttle valve, in order to model turbocharging. Gas temperature was measured just before the intake port and just after the exhaust port by K-type thermocouples. Intake gas temperature T_{in} was regulated by an electric intercooler, followed by an electric heater, placed just before intake. The recirculated exhaust gas went firstly through a Diesel Particulate Filter (DPF) and then was cooled by the EGR water heat exchanger before mixing with the fresh air from the surge tank and entering the supercharger. The intake gas oxygen concentration was measured with a portable oxygen tester (POT-101: SHIMAZU) and regulated by tuning the EGR. The O_2 meter was located just before the intake port.

The exhaust gas composition was inspected with an automotive exhaust gas analyzer (MEXA-1600D: HORIBA) which included the NDIR (non-dispersive infrared sensor) for CO and CO_2 , an FID (Flame Ion Detector) for total hydrocarbon (THC), and a CLD (Chemical Luminescence Detector) for NO_x . The smoke emissions were measured by a Bosh-type smoke meter (AVL-415S: AVL).

Ordinary diesel fuel (JIS No. 3), whose properties are specified in the following Table 2, was used in all experiments.

Fuel denomination	JIS No. 3 Diesel
Density	0.812 g/cm^3
90 % Distillation temperature	336°C
Lower heating value	43.1 MJ/kg
Cetane number	54.2

Table 2: *JIS No. 3 Fuel Specifications*

Fuel injection rates were measured with the Bosch type flow rate meter during some of the real-engine experiments and were subsequently used as input data for the computational simulations.

Designs of the two pistons with respective injector systems which were used in the real

engine experiments and simulations are shown below: the Stepped-lip re-entrant combustion chamber with a single injector (Figure 13) and the Divided combustion chamber with two injectors (Figure 14). Both pistons' outer diameters fit the 85 mm bore. The Stepped-lip re-entrant combustion chamber is combined with a single injector whose sprays' cone angle is 156°, while the Divided combustion chamber is paired with a couple of injectors and sprays' cone angles that vary. In Figure 15 (a) right and left injectors' sprays' patterns are illustrated qualitatively from a top view, while in Figure 15 (b) each spray's cone angle is provided. With respect to the right injector, cone angle is maintained constant and equal to 160°, while in the left injector adopted cone angles are respectively 127° for sprays L1 and L1', 122° for sprays L2 and L2' and 107° for sprays L3 and L3'. Other specifications are shown in Table 3.

Injection system paired with Stepped-lip re-entrant combustion chamber	Φ 0.104 mm x 10 holes (156° cone angle)	
Injection system paired with Divided combustion chamber	Right inj.	Φ 0.125 mm x 6 holes (160° cone angle)
	Left inj.	Φ 0.125 mm x 6 holes (variable cone angle)

Table 3: *Nozzles' specifications*

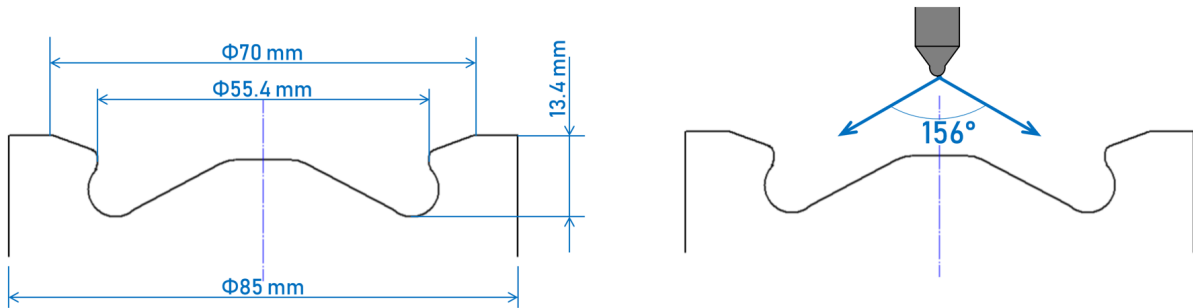


Figure 13: *Stepped-lip re-entrant combustion chamber with single injector*

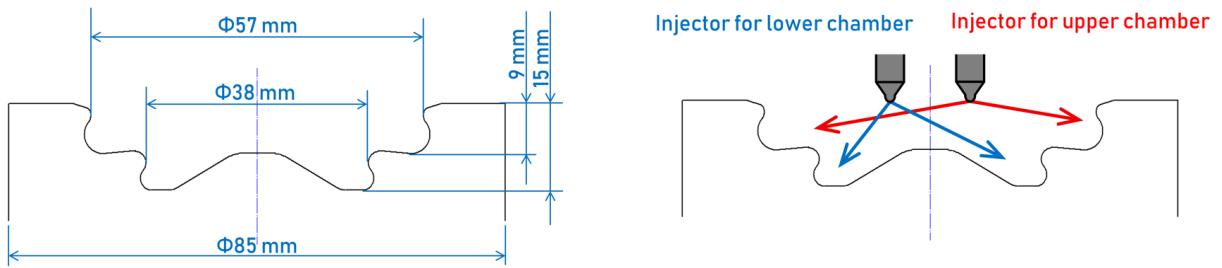


Figure 14: Divided combustion chamber with two injectors

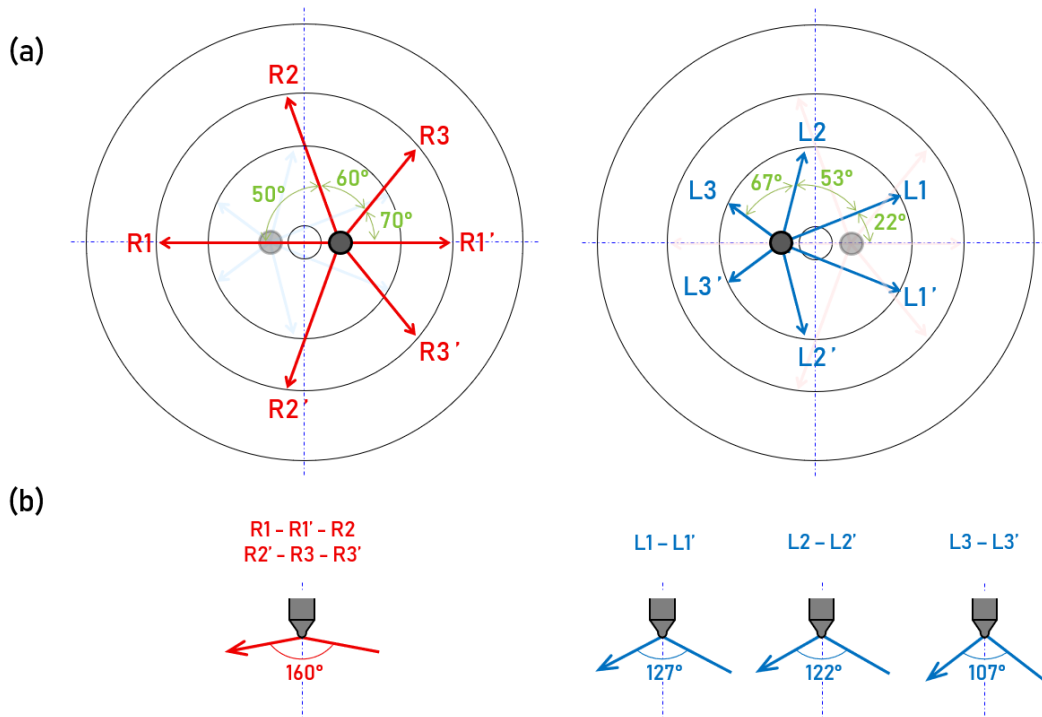


Figure 15: Divided combustion chamber's spray's cone angles

3.2 Software

An Excel code, developed by a team member, was used to collect and reprocess the data obtained from the engine's measurement apparatus. The code was written based on the heat balance equation (Eq.(3)), applied to the closed system of the in-cylinder gas over the engine cycle:

$$W_{i,net} = Q_{fuel} - Q_{ex} - Q_{other} - Q_{unb} - |W_{pump}| \quad (3)$$

where:

$W_{i,net}$: The net-indicated work calculated from the in-cylinder pressure data measurements [$J/cycle$]. The net-indicated work corresponds to the difference between gross indicated work and the pumping work $W_{i,gross} - |W_{pump}|$, which can be calculated from in-cylinder gas pressure data measurements as well: the first one as the work over the period between IVC and EVO, the latter as the work over the period from EVO to IVC;

Q_{fuel} : The total chemical input energy from injected fuel [$J/cycle$];

Q_{ex} : The exhaust energy calculated as the variation in internal energy between the exhaust and intake gases [$J/cycle$]. Intake and exhaust gas temperatures and eight gas components were considered for this calculation;

Q_{other} : The “other energy” calculated from Eq.(3), including the heat transferred to the cylinder wall from IVC to EVO as the main component, and the energy of the unburned fuel diluted into the lubricant oil due to wall wetting with the early fuel injection [$J/cycle$];

Q_{unb} : The energy of the unburned, calculated from the CO and THC contained in the exhaust gases [$J/cycle$];

W_{pump} : The pumping work calculated from the in-cylinder pressure data collected over the exhaust and the intake strokes [$J/cycle$];

It must be noted that, because of the fact that no early injection (injection occurring prior to 25°CA BTDC) was performed in the present study's experiments, the quantity of fuel diluted into the lubricant oil could always be considered negligible. In fact, since the fuel injection was taking place close to TDC, not invading the squish region but directly entering the combustion chamber bowl, impingement on the cylinder wall did not occur. This said, in the experiments, Q_{other} resulted to be virtually coincident with Q_{wall} .

Figure 16 is a visual representation of the just outlined heat balance.

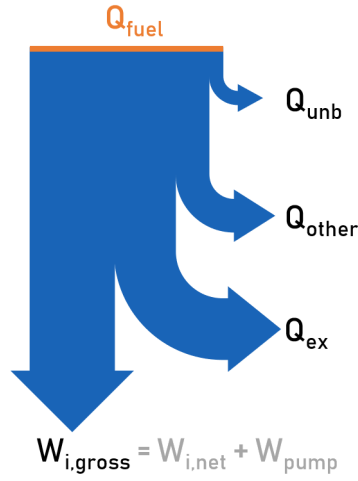


Figure 16: Heat balance diagram

In addition, through the Excel code, some thermal efficiency related parameters were successively obtained from the heat balance components. They are the following:

$$\eta_{i,net} = \frac{W_{i,net}}{Q_{fuel}} \quad (4)$$

$$\eta_u = \frac{(Q_{fuel} - Q_{unb})}{Q_{fuel}} \quad (5)$$

$$\phi_{unb} = \frac{Q_{unb}}{Q_{fuel}} \quad (6)$$

$$\phi_{ex} = \frac{Q_{ex}}{Q_{fuel}} \quad (7)$$

$$\phi_{pump} = \frac{W_{pump}}{Q_{fuel}} \quad (8)$$

$$\phi_{wall}^* = \frac{(Q_{fuel} - W_{i,net} - Q_{ex} - Q_{pump} - Q_{unb})}{Q_{fuel}} \quad (9)$$

$$\eta_{glh} = \frac{W_e}{W_o} \quad (10)$$

where:

- $\eta_{i,net}$: Net-indicated thermal efficiency [%];
- η_u : Combustion efficiency [%];
- ϕ_{unb} : Unburned loss ratio [%];
- ϕ_{ex} : Exhaust loss ratio [%];
- ϕ_{pump} : Pumping loss ratio [%];
- ϕ_{wall}^* : Heat transfer loss ratio [%];
- η_{glh} : Degree of constant volume [%], corresponding to the ratio between the theoretical work obtained from the heat release at each crank angle, W_e , and the theoretical work obtained from Otto cycle, W_o , during the heat release period;

Combustion noise (CN) was calculated from the in-cylinder pressure level (frequency characteristic), Eq. [11], to which the Structural Attenuation (SA) specific of the test engine was added. An averaged structural damping (frequency characteristic) had been previously obtained from multiple experimental test conditions.

In-cylinder pressure level was obtained as:

$$CPL = 10 \cdot \log_{10} p^2 \quad [dB] \quad (11)$$

Combustion noise is given by the equation:

$$CN = CPL + SA \quad [dBA] \quad (12)$$

For a deeper understanding of the combustion characteristics, numerical simulations of the combustion processes were carried out with the help of a 3D CFD software: AVL FIRE v2014.

1.

4 PART 1: Comparison of partially premixed diesel combustion and conventional diesel combustion

4.1 Experimental Procedure

4.1.1 Comparison between partially premixed and conventional diesel combustions

The object of the first experimental experience was the comparison of the partially premixed combustion with the conventional diesel combustion strategy. The pilot-pilot-main strategy was adopted for the conventional diesel combustion, (Figure 17, (a)), while, for the partially premixed combustion, a two-stages heat release was generated, with a pre- and a primary injection contributing to the first, premixed-like combustion stage and a secondary injection contributing to the second, mixing-controlled combustion stage (Figure 17, (b)).

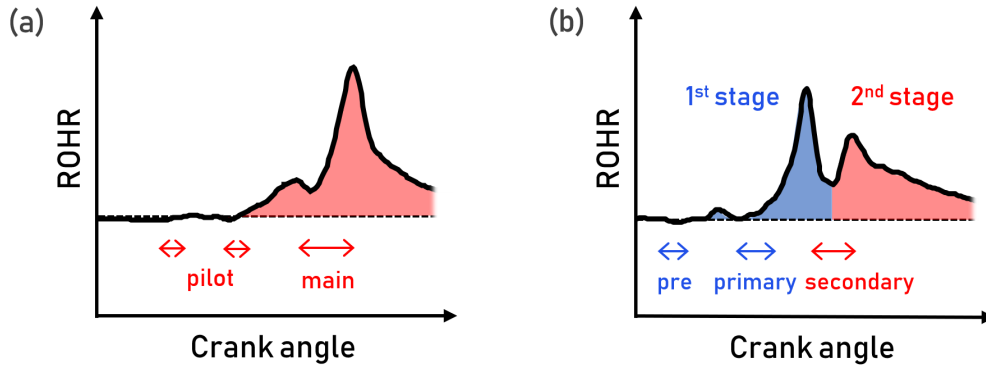


Figure 17: (a) Pilot-pilot-main Diesel Combustion; (b) Partially Premixed Diesel Combustion with triple fuel injection

Both strategies were performed at three different engine loads: low load (IMEP ≈ 0.4 MPa and engine speed = 1500 rpm), medium load (IMEP ≈ 0.7 MPa and engine speed = 2000 rpm) and high load (IMEP ≈ 1.1 MPa and engine speed = 2000 rpm). Load was controlled by changing the fuel quantity Q_{total} injected per cycle from 10 mg/cycle (low load) to 18 mg/cycle (medium load) and, lastly, to 30 mg/cycle (high load). Fuel injection pressure was also changed (increased) with load: values are reported in Table 4 together with the injection timings.

Settings for the conventional diesel combustion were chosen according to the reference values indicated by the Japanese Strategic Innovation Promotion Program (SIP [23]). On the other

hand, with regard to the partially premixed operating parameters, a study from professor Ogawa et al.[22] was considered as the starting point. In the study, a two-stage heat release combustion with the first premixed-like flame and the second mixing-controlled flame is analysed at a medium load condition; an optimization of the first fuel injection quantity and of the second fuel injection timing was carried out in order to gain the highest indicated thermal efficiency and the minimum engine noise. Successively, our team conducted a further optimization of the results of this research, by splitting the first fuel injection into two smaller injection events, aiming at lowering the combustion noise while maintaining the high thermal efficiency. The best performances were obtained for a 50% - 50% fuel quantity distribution among the pre- and the primary fuel injections, which contribute to the first combustion event.

Intake gas pressure p_{in} , intake gas temperature T_{in} and intake oxygen concentration O_{2in} , were varied with load but maintained equal within the two combustion strategies. Coolant temperature was maintained at 80°C and swirl ratio at 1.6 for all conditions.

In the following Table 4 all experimental conditions are summarized.

Combustion type	Partially premixed	Conventional diesel	Partially premixed	Conventional diesel	Partially premixed	Conventional diesel	U.M.
Engine load	Low load		Medium load		High load		–
Engine speed	1500		2000		2000		[rpm]
Total fuel quantity, Q_{total}	10		18		30		[mg/cycle]
IMEP	≈ 0.4		≈ 0.7		≈ 1.1		[MPa]
Fuel injection pressure	100		200	135	200		[MPa]
Pre / First pilot injection quantity	3	1.5	4.5	1.5	–	1.5	[mg/cycle]
Primary / Second pilot injection quantity	3	1.5	4.5	1.5	4	1.5	[mg/cycle]
Secondary / Main injection quantity	4	7	9	15	26	27	[mg/cycle]
Pre / First pilot injection timing	- 13	- 10	- 10	- 14	–	- 20	[°CA ATDC]
Primary / Second pilot injection timing	- 7	- 2.75	- 2.5	- 3	- 6.75	- 12	[°CA ATDC]
Secondary / Main injection timing	1.75	4	2.5	4.5	- 2	2	[°CA ATDC]
Intake gas pressure, p_{in}	102		120		160		[kPa abs.]
Intake oxygen concentration, O_{2in}	15.5		16.5		17.0		[vol.%]
EGR ratio	44.5		34.0		24.2		[%]
Intake gas temperature, T_{in}	60		40		40		[°C]
Swirl ratio	1.6						–
Coolant and lubricant temperature	80						[°C]
Combustion chamber	Re-entrant (Stepped-lip)						–
Compression ratio (Geometrical)	16.3						–

Table 4: *Experimental conditions*

4.1.2 Influence of combustion phase

Effects of advancing and retarding the combustion phase at low and at high engine loads were then analysed.

The crank angle at which 50% of the heat has been released by the fuel over one cycle is here denominated CA50. By advancing or retarding the injections timings while maintaining dwell timings constant, CA50 was changed at low and high loads between 5°CA ATDC and 11°CA ATDC, for both combustion strategies (Table 5). Other settings were maintained constant.

	Partially premixed			Conventional			U.M.
CA50 (Low load)	5.4	8	10.8	4.4	7.4	10.6	[°CA ATDC]
CA50 (High load)	6.6	8.6	10.6	6.2	8.6	11	[°CA ATDC]

Table 5: CA50 settings for the study of combustion phase

4.1.3 Influence of EGR ratio on partially premixed combustion

Successively, considering again the original settings (most advanced combustion phase for premixed combustion and most retarded combustion phase for conventional combustion), effect of EGR was studied: higher EGR rates were enforced in partially premixed combustion in order to even the levels of NO_x emissions with the ones of the conventional diesel combustion. The feedback in terms of thermal efficiency and of smoke emissions was collected. This was done for all of the three load conditions.

4.1.4 Computational investigation of combustion mechanism at low engine load

Further investigation of the combustion process was carried out by means of CFD simulation on the software AVL FIRE v2014. 1. In particular, it was searched the mechanism of improvement of the thermal efficiency of partially premixed combustion at low load conditions.

Figure 18 shows the computational mesh of the Stepped-lip re-entrant combustion chamber. In this case, in order to reduce the calculation time, a 36° sector mesh was adopted (given the symmetry of the behaviour of in-cylinder gasses employing a ten-holes nozzle).

A 0.5 mm average cell size was set, and the total number of resulting cells was around 172000. Table 6 shows the sub-models for the spray¹, turbulence², mixture formation³, chemical reaction⁴, and heat transfer⁵.

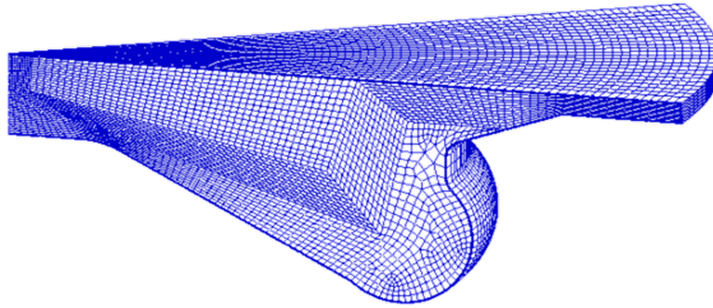


Figure 18: Computational mesh of 1/10 sector of the Stepped-lip re-entrant combustion chamber

Spray	Discrete droplet model
Evaporation	Dukowitz ¹
Breakup	KH-RT ¹
Turbulence	$K - \xi - e$ model ²
Turbulence interaction	PDF - Hybrid ³
Chemical interaction	Tsurushima ⁴
Heat transfer model	Han-Reitz model ⁵

Table 6: Sub-models in CFD code FIRE

The investigated alternatives were: the conventional combustion at the most advanced and at the most retarded CA50 (CA50 = 4°CA ATDC and CA50 = 10°CA ATDC), and the partially premixed combustion at the most advanced CA50 (CA50 = 5°CA ATDC). Particular attention was paid to the gasses temperature and heat flux distributions at the wall.

4.2 Results and Discussion

4.2.1 Comparison between partially premixed and conventional diesel combustions

Obtained plots of in-cylinder pressure, temperature and rate of heat release versus crank angle are depicted in Figure 19.

From the comparison between the ROHR and the corresponding pressure plots it can be seen how the earlier combustion of the PPCI causes an earlier pressure rise, and higher pressure peak values with respect to the conventional diesel combustion. In-cylinder gas temperature also increases earlier for PPCI, reaching as well slightly higher peak values.

Looking at PPCI strategy, the first two injections (pre- and primary) for low and medium load conditions, and the first injection (single primary) for high load condition, they all contribute to the first peak of heat release, and they are completed before the start of ignition, supposedly producing a premixed flame. The third or the last injection is responsible for the second peak of heat release and it occurs contemporary to a presumed mixing-controlled flame. In this way the energy release rate results split in these two stages, which reach almost equal peak values.

On the other hand, it is possible to observe the effects of the pilot injections on the conventional diesel combustion: they reduce the premixed stage and promote the release of most of the fuel energy during the diffusion stage.

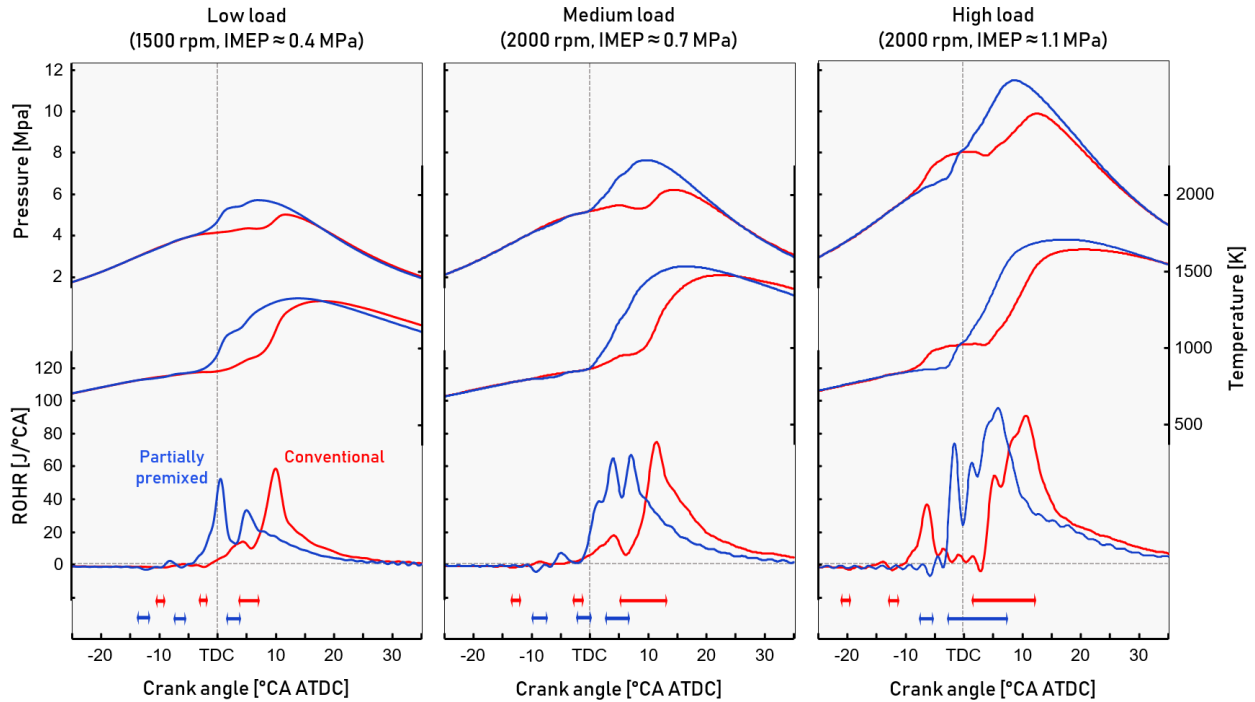


Figure 19: Comparison of pressure, temperature and Rate Of Heat Release versus Crank Angle among partially premixed combustion and conventional diesel combustion

The heat balance depicted in Figure 20 shows that, at all the three load conditions, the gross indicated work resulting from PPCI is higher than the one of conventional diesel combustion: plus 1.6 % at low load, plus 2.5 % at medium load and plus 0.8 % at high load. These increments correspond parallelly to relative higher degrees of constant volume, clearly due to the combustion phase being closer to TDC in the PPCI case.

Some considerations can be made about the other two main portions in the heat balance: the cooling loss and the exhaust losses. Exhaust loss, which accounts for about 30 % in the heat balances, is lower at every load for the PPCI condition. This can easily be justified by the advanced phase of the combustion: the exhaust gasses' temperatures are slightly lower because of the earlier start of the energy release in the cycle. On the other hand, cooling loss does not have an unique behaviour among engine loads. At high load, cooling loss increases from conventional to PPCI, while at medium and low loads it stays almost constant. Cooling loss is due to the wall heat exchange and depends strongly on the in-cylinder gasses' local temperature distribution. Later in this study, computational simulations which reveal wall temperature and

heat flux distribution have been carried out for similar working conditions, to investigate in detail this mechanism.

Finally, unburned loss calculated from the CO and THC content in the exhaust gasses shows an increase at low load, a slight decrease at high load and a halving at medium load from conventional combustion to partially premixed combustion. However, it should be noted that, at medium load, fuel injection pressure is different among the two strategies (200 MPa for PPCI and 135 MPa for conventional diesel combustion) and it is known that fuel injection pressure has a very strong influence on combustion characteristics.

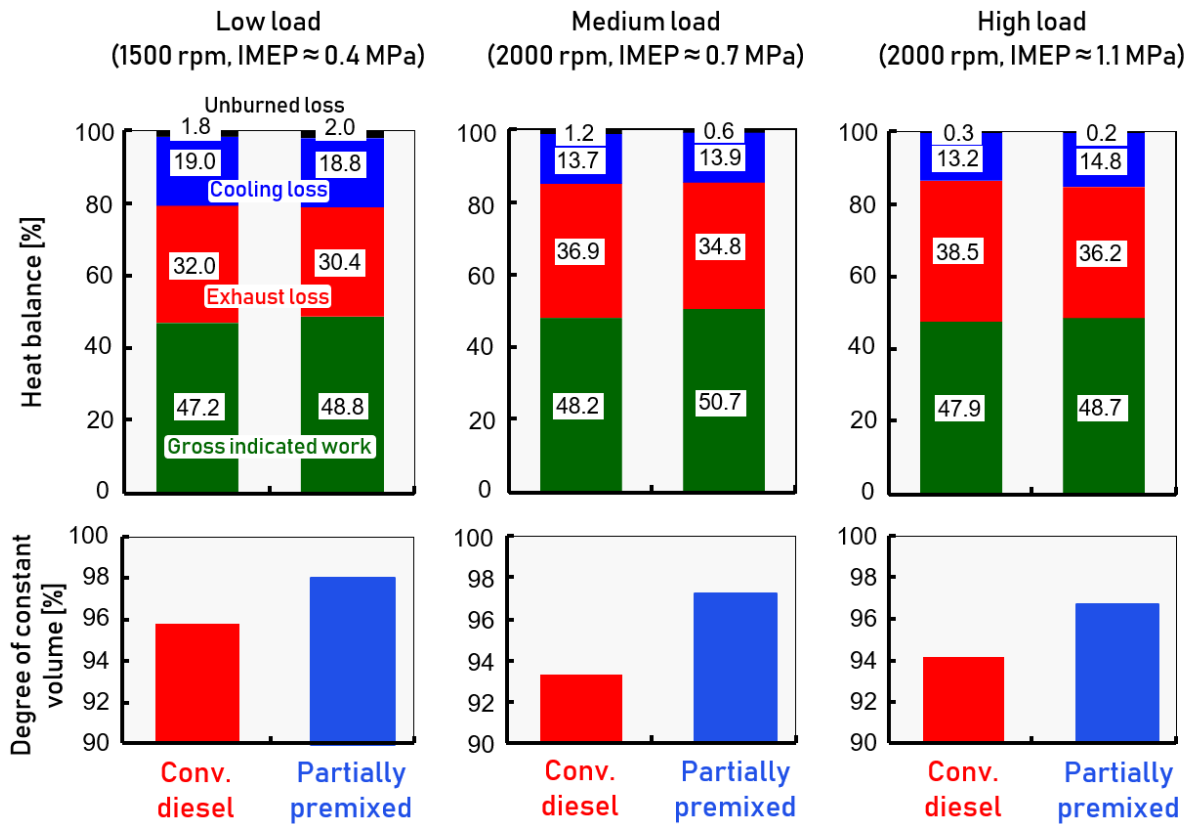


Figure 20: Heat balance and degree of constant volume of conventional and partially premixed diesel combustion at three engine loads

Moving on to the analysis of combustion noise and emissions, in Figure 21 are depicted: the maximum rate of pressure rise ($dp/d\theta_{max}$), the combustion noise (CN) and the measured NO_x and smoke emissions.

The early combustion of PPCI naturally brings with it an higher maximum rate of pressure rise, and pressure peak values and therefore of the combustion noise. However, it should be noted that the gap with conventional combustion is kept within 1 dBA at high load and within 1.8 dBA at low and medium loads, and, therefore, it does not represent a criticality.

The increase in NO_x emissions with load for both combustion methods is directly related to the increase in maximum burning temperature, with larger amounts of charge being in the temperature range of formation of NO_x (see Kamimoto map - Figure 8). In a similar way, the greater peak temperatures reached by PPCI translates in relative higher NO_x rates with respect to conventional combustion.

Finally, smoke emissions are considered: lower values result for PPCI, and a trade-off relationship with NO_x is verified among the different engine loads. At medium load, smoke emissions are higher than at low and high load for both injection strategies, and the gap between smoke emission values of conventional and partially premixed combustion is wider. This might have possibly been influenced by the difference in fuel injection pressure, as previously mentioned.

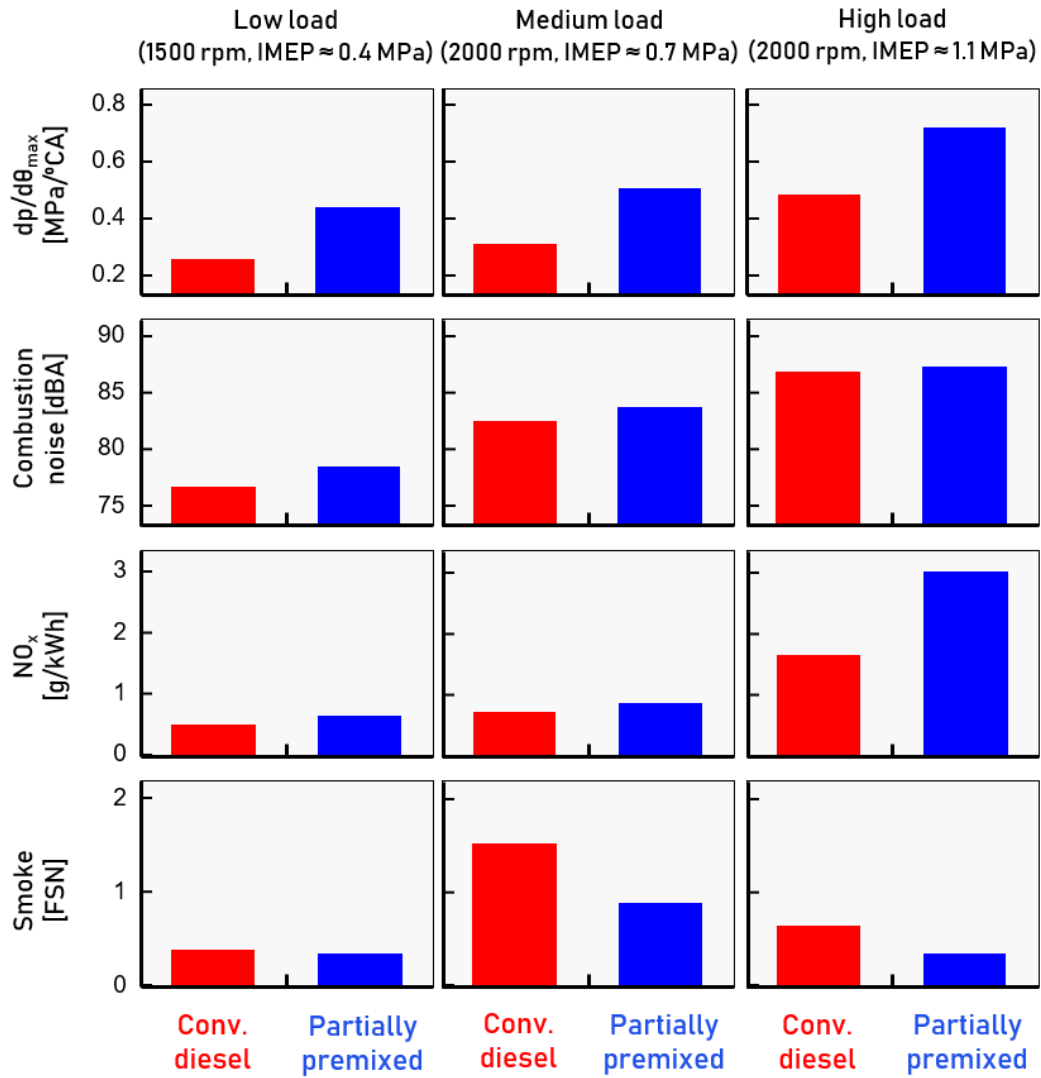


Figure 21: Maximum rate of pressure rise, combustion noise, NO_x and smoke emission levels of conventional and partially premixed diesel combustion at three engine loads

4.2.2 Influence of combustion phase

The effect of combustion phase on ROHR, in-cylinder pressure and temperature on both conventional and partially premixed combustion at low and at high load is shown in Figure 22. Solid lines indicate the data from the original settings. It can be observed that everywhere combustion becomes closer to TDC, it produces earlier and, in general, higher-peaked ROHRs, pressures and temperatures.

The influence of the change in the combustion phase on thermal efficiency related parameters is reported in Figure 23. Effects on both PPCI and conventional combustion are shown in each plot for comparison. Data resulting from the original settings are indicated with full markers: CA50 set at around 5 and 7°CA ATDC for PPCI, respectively at low and high loads, and CA50 set at around 11°CA ATDC for conventional diesel combustion both at low and high loads.

Combustion efficiency, η_u , does not change significantly with phase or among injection strategies and is maintained high at all conditions. Values around 98 % are obtained at low load, at which combustion temperatures are inherently lower, and values very close to 100 % result at high load, at which temperatures are typically higher.

The net indicated thermal efficiency, $\eta_{i,net}$, shows an increasing trend with the advancement of the combustion phase, regardless of the injection strategy. The same trend is found for the degree of constant volume. While the latter is independent from the combustion strategy, the net indicated thermal efficiency stands slightly higher at every CA50 condition for PPCI. This gap is wider at low loads and very contained at high loads. The trend of the net indicated thermal efficiency can be interpreted by the combined effect of reduction the exhaust loss and the increase of the cooling loss. At low load, the PPCI's higher net indicated thermal efficiency with respect to conventional diesel combustion results, at all CA50 conditions, from the combination of smaller exhaust losses and almost equal cooling losses. At the most advanced phase the cooling loss of conventional diesel combustion is considerably higher than PPCI and this peculiar condition has been further investigated by means of computational simulation and it is reported in the next section of this report. At high load, since the lower exhaust

loss of PPCI combustion is balanced by the higher cooling loss, difference with conventional combustion in net indicated thermal efficiency is small.

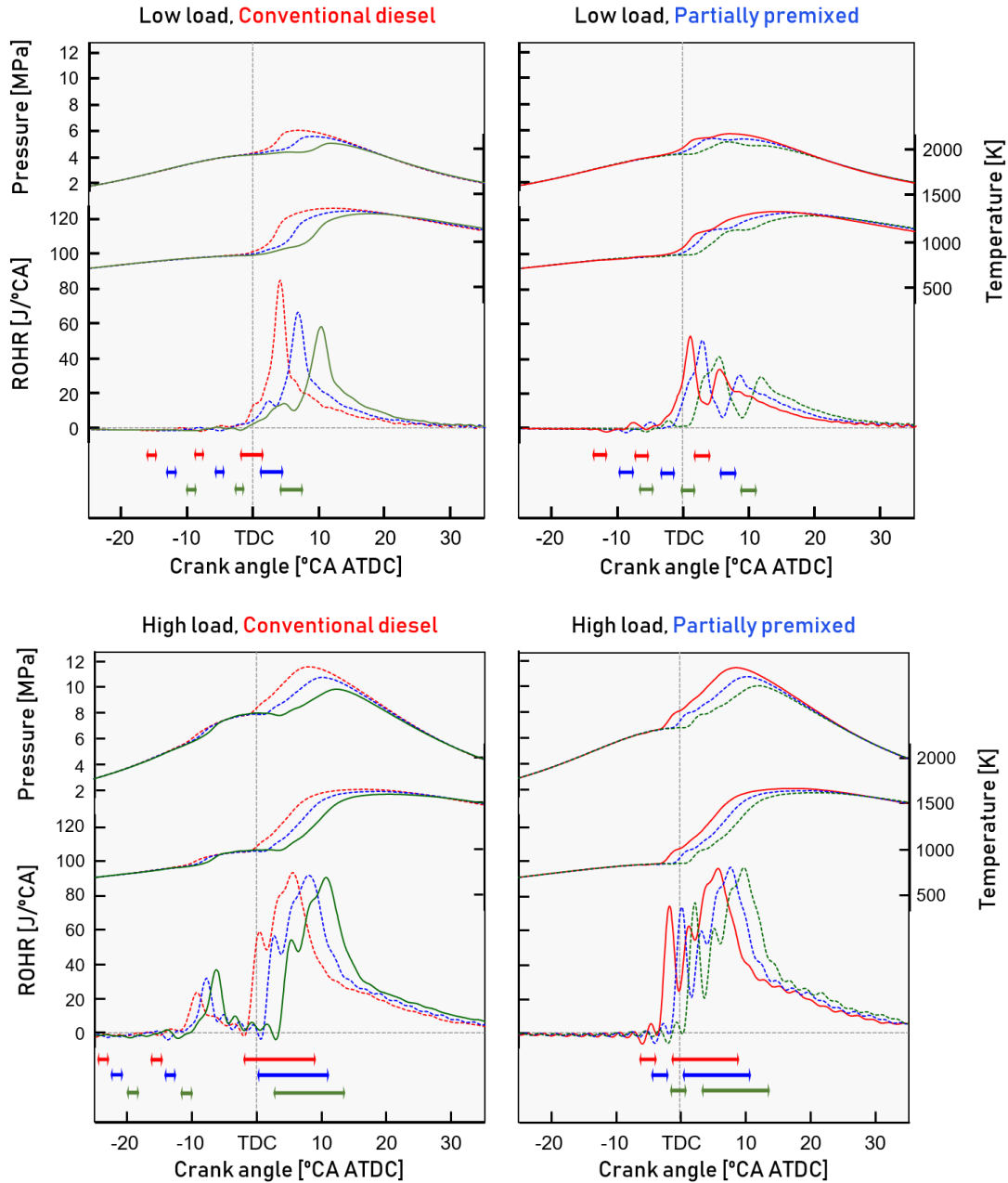


Figure 22: Pressure, temperature and ROHR plots for different combustion phases, at low and high loads, for Conventional Diesel Combustion and for Partially Premixed Diesel Combustion

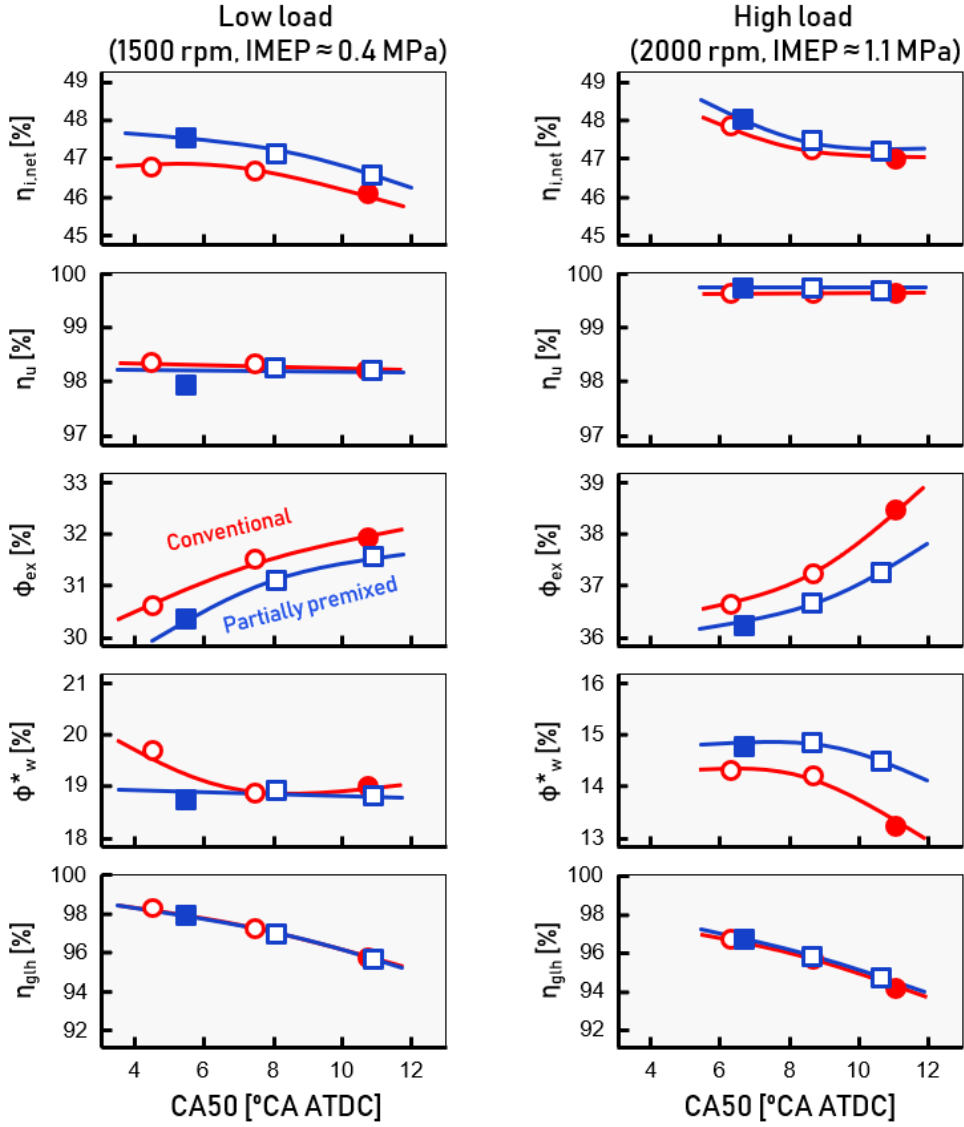


Figure 23: Thermal efficiency related parameters evaluated at different combustion phases and engine loads for Conventional Diesel Combustion and Partially Premixed Diesel Combustion

In Figure 24 the maximum pressure increase rate ($dp/d\theta_{max}$) is portrayed along with combustion noise, and NO_x and soot emission levels.

At low load, with the advancement of the combustion phase, $dp/d\theta_{max}$ increases both for PPCI and conventional diesel combustion. CN follows a similar trend. At the most advanced CA50 condition, both $dp/d\theta_{max}$ and CN are higher for conventional diesel combustion. On the other hand, at high load condition, in spite of the higher level of maximum pressure increase rate for PPCI, CN are relatively comparable among the two strategies. Typically, in a case

when a reduction of the engine noise is wanted, the implementation of a late combustion can be effective: this is proved by the just-obtained results. It must be noted, however, that this strategy is effective at low load, where reaction speed is lower, but not at higher load, where reaction speed is higher. In fact, it is possible to notice that despite of the gap in the maximum rate of pressure rise, the combustion noise is comparable among the two strategies at high engine load.

In Figure 24, NO_x and smoke emissions are plotted as well as a function of CA50. It is clear that NO_x emissions' trend is influenced exclusively by the phase rather than by the type of combustion, and that low smoke and high NO_x emissions in the original PPCI combustion are a direct consequence of the early combustion phase.

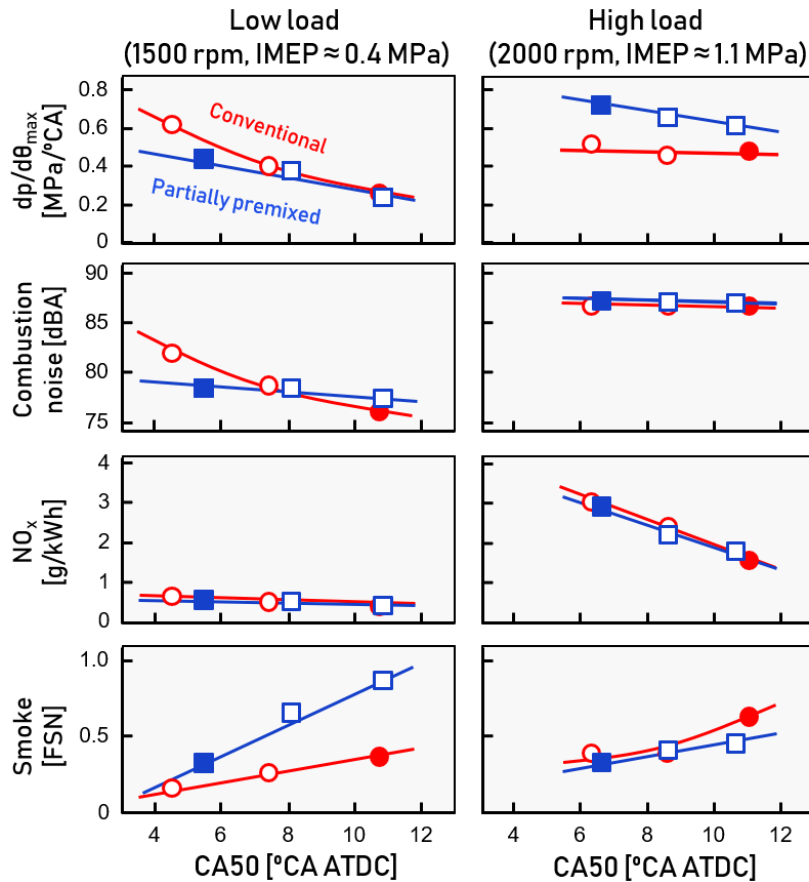


Figure 24: Maximum rate of pressure rise, combustion noise, and NO_x and Particulate emissions obtained at different combustion phases, at low and high engine loads, for Conventional Diesel Combustion and for Partially Premixed Diesel Combustion

4.2.3 Influence of EGR ratio on partially premixed combustion

Gross thermal efficiency and smoke emissions versus NO_x emissions are reported in Figure 25. Full markers represent the original conditions (original settings for conventional and for partially premixed) while the different shapes indicate the engine load. By diminishing the oxygen content in partially premixed combustion, NO_x were decreased to the same NO_x levels shown by the conventional diesel combustion.

In the case of thermal efficiency, slightly lower values at low and high loads and slightly higher values at medium loads resulted, with no sensible difference from the previous condition. Thermal efficiency of partially premixed combustion was still surpassing that of conventional diesel combustion.

Regarding smoke emissions, while at medium and low load the increment was contained and kept below conventional combustion's levels, at high load a big increment was recorded. At the same NO_x emission level, smoke emissions are higher than conventional diesel combustion, suggesting that improvements should still be achieved to make PPCI performances competitive at high loads.

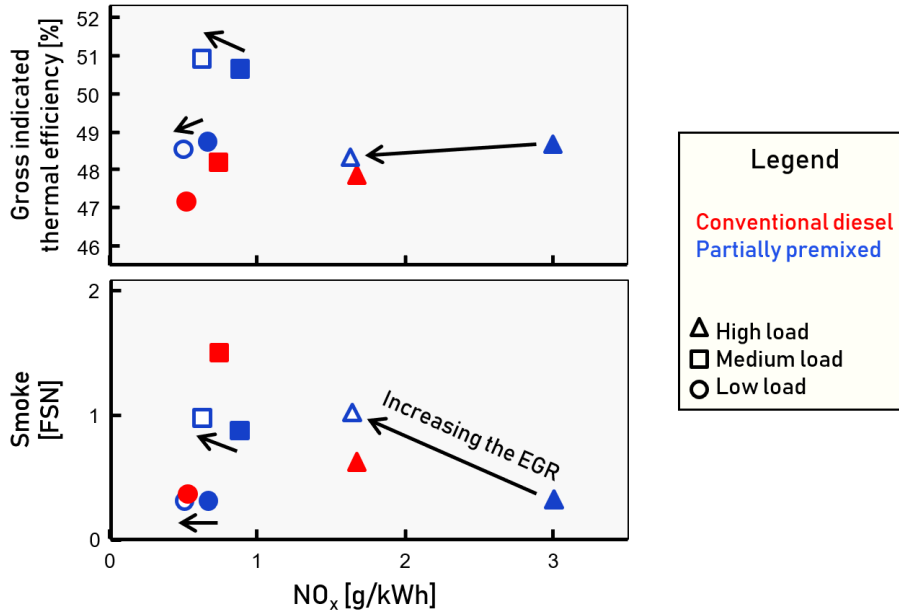


Figure 25: NO_x reduction by EGR, with effects on emissions and thermal efficiency, for Partially Premixed Diesel Combustion

4.2.4 Computational investigation of combustion mechanism at low engine load

Computational simulations conducted of the most advanced of CA50 conditions for both partially premixed and conventional combustion, and most retarded CA50 condition for conventional combustion are now presented.

Firstly, pressure and ROHR versus crank angle are displayed in Figure 26 for a qualitative comparison. The fuel injection rate (measured with a Bosh flow meter and subsequently in simulation) is included in the lower part of the graph. It can be attested how the simulation reproduces the combustion process (ignition delay, ROHR, pressure pattern) relatively well.

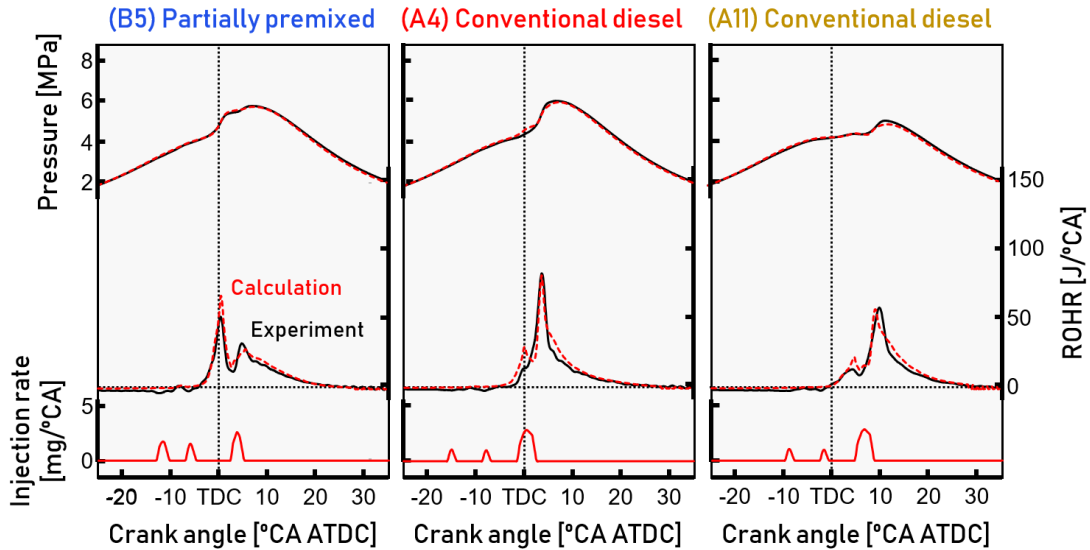


Figure 26: *Affidability of calculation results*

Secondly, in Figure 27 cooling loss rate versus crank angle is reported. Similar patterns are shown for the two conventional combustion strategies: a single step increment to a peaking value which, in both cases, is higher than that of PPCI. On the other hand, the PPCI strategy reveals a two-step increase in the rate of cooling loss: each one caused by one of the heat release stages.

Figure 28 shows the gas temperature and heat flux at the combustion chamber wall. These are a visual explanation of the rates of cooling loss of Figure 27. Considering the two early CA50 combustion strategies, it is possible to see how the gas temperature of conventional combustion near the wall is generally higher than that of PPCI at a larger area. A similar trend is exhibited

by the heat flux at the wall all along the combustion process. At 4° CA ATDC, heat flux is more intense for conventional combustion as it is already reaching its peaking rate, while PPCI shows its heat flux peak at around 8° CA ATDC.

These results indicate that by splitting the total fuel injected amount in such a way that the chemical energy release is divided in two phases, spray penetration is reduced and, consequently, less fuel is burning closer to the combustion chamber wall.

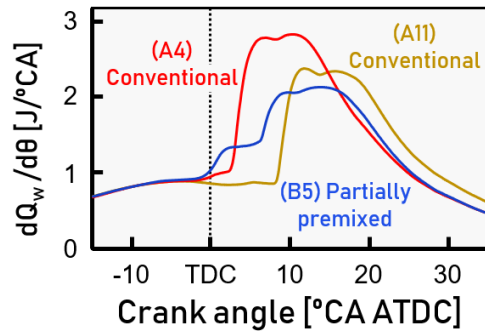


Figure 27: Rate of cooling loss over the crank angle of the most advanced cases of Conventional and Partially Premixed combustions and of the most delayed case for Conventional combustion

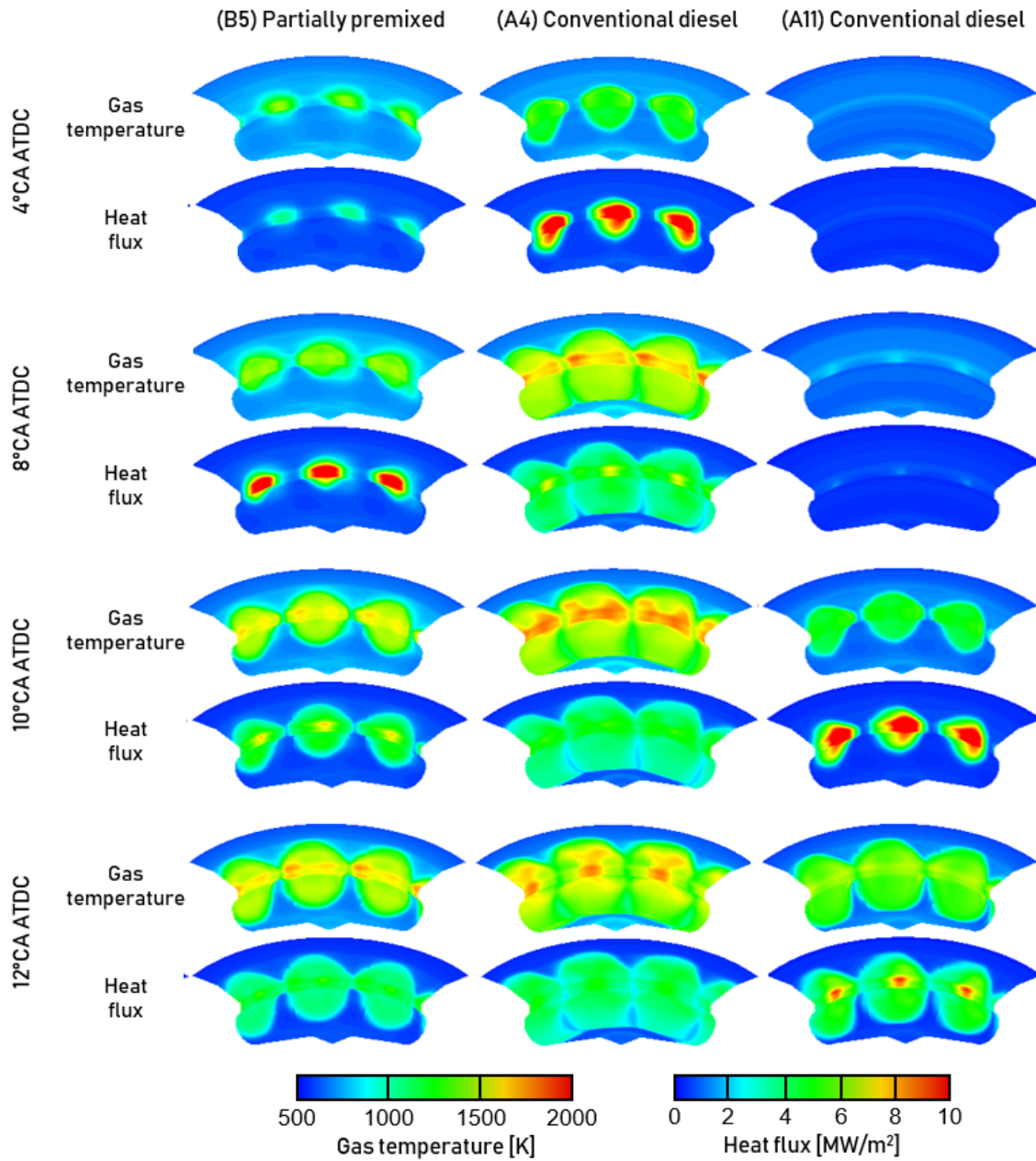


Figure 28: Visualization of in-cylinder gas temperature and heat flux evolution at the combustion chamber's wall

5 PART 2: Enhanced air utilization through spray-dividing combustion chamber design

5.1 Overview of the divided combustion chamber concept aimed at an improved air utilization

5.1.1 Previous study on the divided combustion chamber concept

In section 4.2.3 it was demonstrated that, at high load, the smoke emissions were much higher for PPCI, compared to conventional combustion, when the same level of NO_x was established by the effect of EGR. In order to improve this point and enhance PPCI's performance at high load, a new concept of combustion chamber and injection apparatus was introduced. The starting point was the consideration that smoke formation is promoted when a late fuel spray enters and burns in the high temperature / low O_2 region left by the first fuel spray combustion (Figure 29, (a)). With the new concept, an attempt is made to keep separated these two regions: the chamber design together with the injection strategy are key points. A lip is introduced dividing the chamber in two parts (Figure 29, (b)) in such a way that an early first fuel injection would enter the upper one while a second injection would enter the lower one. In order to avoid the invasion of the lower chamber by the first fuel injection, its timing must be sufficiently advanced. On the other hand both injections occur near TDC when a traditional Re-entrant combustion chamber is utilized.

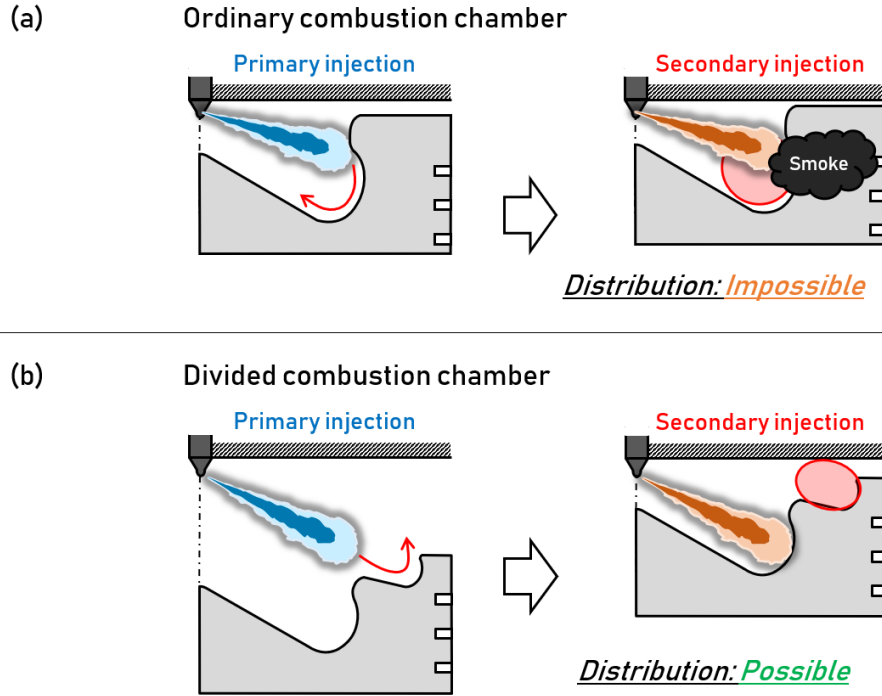


Figure 29: Concepts of combustion in the standard Re-entrant combustion chamber (a), and combustions' spatial separation in a Divided combustion chamber (b)

The results of a study on the new concept will be here presented briefly as an introduction for the last chapter. Here, only the results of real-engine experiments conducted in the study will be discussed.

The geometry of the two utilized combustion chambers is shown in Figure 30.

Due to the necessary early injection, the compression ratio of the Divided combustion chamber had to be decreased to fourteen, in order to avoid early ignition. For a fair comparison the compression ratio of the Re-entrant combustion chamber was also set to fourteen.

Experimental conditions were: high load (IMEP between 0.8 and 1.2 MPa and engine speed equal to 2000 rpm), total fuel quantity Q_{total} varying from 25 to 32 mg/cycle and intake oxygen concentration changed by means of EGR between 11% and 17%. Double injection strategy with the first injection timing $\theta_{1st} = -35^\circ CAATDC$ and the second injection timing $\theta_{2nd} = -5^\circ CAATDC$ was carried out on both combustion chambers.

The ROHR obtained at the best thermal efficiency condition, (namely 44.6% with $Q_{total} = 25mg/cycle$ and O_2 concentration set at 13%), smoke emission levels and thermal efficiency

values are provided in Figure 31.

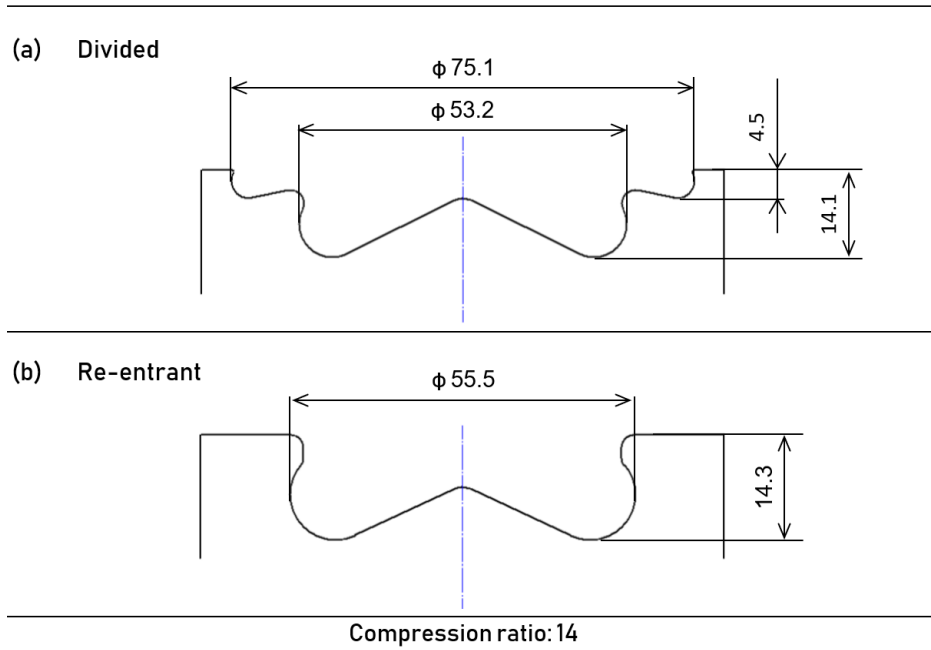


Figure 30: Designs of Divided (a) and Re-entrant (b) combustion chambers

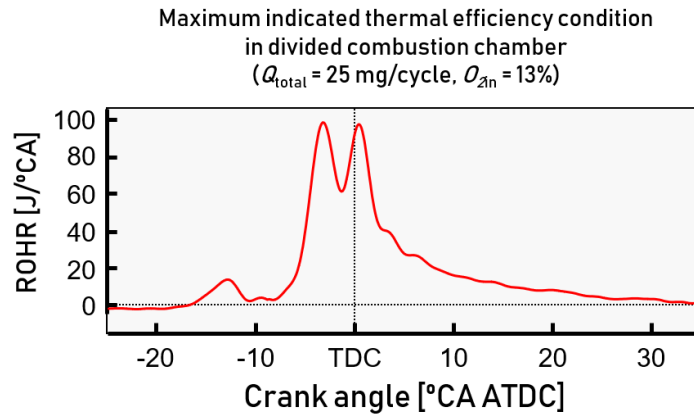


Figure 31: Rate of heat release in the Divided combustion chamber

Regardless of the Q_{total} , the Smoke - NO_x trade-off was confirmed in both chambers and in the Divided chamber it appeared to be slightly improved (Figure 32). It is clear from these data that smoke reduction can be achieved with the implementation of the Divided combustion chamber even at medium and high loads. In this particular case, the highest reduction was achieved at the highest Q_{total} condition. This suggests that the fuel spray spatial separation

(reduction of the interference between the first and the second spray combustion events) was established even under high load conditions.

With regards to the thermal efficiency, the Divided chamber clearly showed higher values than the Re-entrant chamber's ones at all Q_{total} settings. However, its maximum value resulted to be just of 44.6%, which is not competitive with the optimized values obtained in the PART 1 of this report. The causes are believed to be the lower compression ratio, which was needed to ensure the combustion delay, and the lower degree of constant volume due to the early combustion.

In conclusion, from this study it was suggested the necessity of a method for retarding the combustion phase, shifting it closer to TDC, in order to increase the combustion efficiency, while maintaining the fuel sprays' separation effect.

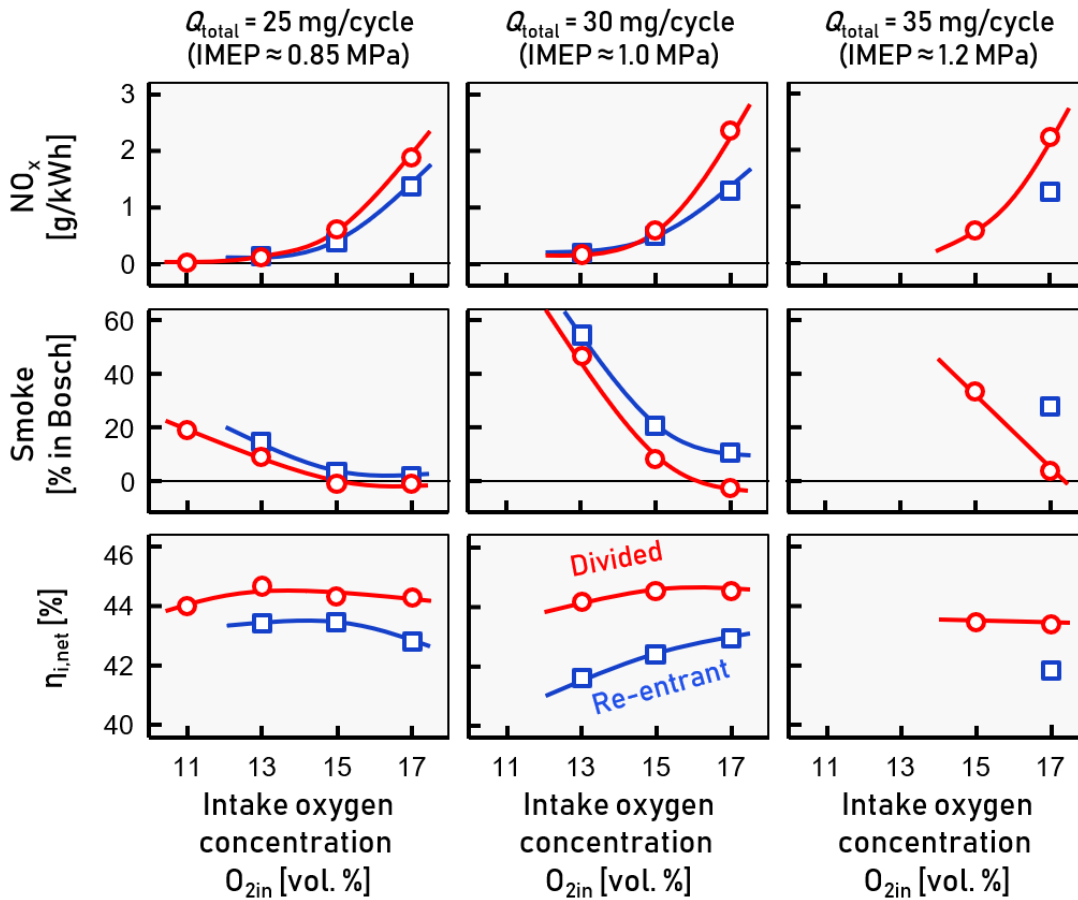


Figure 32: NO_x and Particulate emissions and net indicated thermal efficiency as functions of the intake oxygen concentration, for the PPCI with the Divided and the Re-entrant combustion chambers

5.1.2 Current study on the divided combustion chamber concept

Starting from the conclusions of the study presented in the previous paragraph, a new combustion chamber and injection system are here proposed. Improvements in terms of combustion efficiency by increased compression ratio while maintaining fuel sprays combustions separated were attempted.

The main issue related to the first model of the Divided combustion chamber was the strongly advanced first fuel injection timing. This was necessary because of the narrow injector cone angle (Figure 33 (a)). If a wider cone angle would have been used, in fact, the combustion separation would not have been possible, as visually explained in Figure 33 (b).

In the newly proposed concept, this issue is solved by a variable cone angle between the first and the second fuel injections. In this way the first one is performed with a wider cone angle and enters the upper combustion chamber region without requiring an advanced timing, while the second one is performed with a more narrow cone angle, avoiding the invasion of the upper part of the combustion chamber (conceptual scheme is displayed in Figure 33 (c)). The order of the injections could possibly be exchanged.

The variable cone-angle can be achieved in practice with the implementation of two independent injectors, as shown in Figure 34.

In conclusion, this new concept eliminates the need for an early injection and a consequent long combustion delay and therefore for a lower compression ratio. This latter one can be set again to 16.3, as it was in PART 1 of this study, where the Stepped-lip re-entrant combustion chamber was utilized. Both combustion events can take place close to TDC (not necessarily in the same order as in the conceptual examples) and higher thermal efficiency is expected.

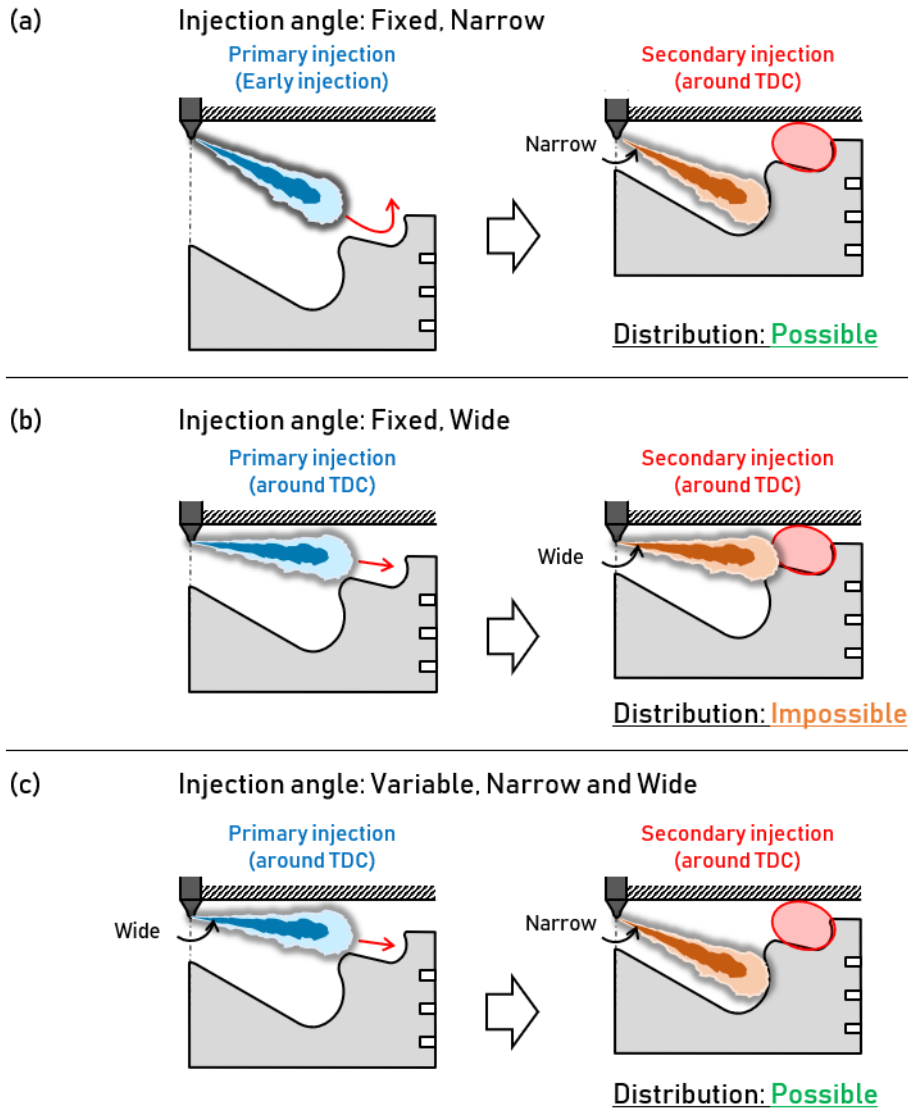


Figure 33: Concept of divided combustion chamber where injection angle is: (a) fixed and narrow, (b) fixed and wide, or (c) variable

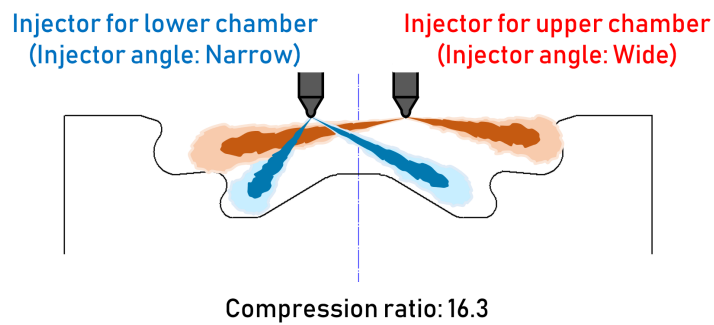


Figure 34: New Divided combustion chamber design and double injector system

5.2 Experimental procedure

Computational simulations using the software AVL FIRE v2014 were conducted on the implementation of partially premixed combustion in the Stepped-lip re-entrant combustion chamber and in the new Divided combustion chamber. Results were compared also with real-engine experiments on the Stepped-lip re-entrant chamber.

The new Divided chamber layout is included in the Experimental Apparatus chapter in Figures 14 and 15, and the Stepped-lip re-entrant combustion chamber's one is depicted in Figure 13.

The real-engine parameters which were taken also as calculation settings are displayed in Table 7.

Engine speed [rpm]	2000
Total fuel injection quantity, Q_{total} [mg/cycle]	20
Indicated mean effective pressure, IMEP [MPa]	≈ 0.8
Primary injection quantity, Q_{1st} [mg/cycle]	5.4
Secondary injection quantity, Q_{2nd} [mg/cycle]	14.6
Primary injection timing, θ_{1st} [°CA ATDC]	-7.25
Secondary injection timing, θ_{2nd} [°CA ATDC]	-0.25
Fuel injection pressure [MPa]	200
Intake gas pressure, p_{in} [kPa abs.]	140
Intake oxygen concentration, O_{2in}	15 %
Intake gas temperature, T_{in} [°C]	40
Swirl ratio	1.6
Coolant and lubricant temperature [°C]	80
Compression ratio (Geometrical)	16.3

Table 7: *Experimental conditions for the computational simulations of the Partially Premixed Combustion*

The medium-high load corresponding to an engine speed of 2000 rpm and an IMEP of about 0.8 MPa was achieved with a fuel injection quantity of 20 mg/cycle. Fuel injection pressure was set at 200 MPa, intake gas pressure p_{in} at 140 kPa and intake gas temperature T_{in} at 40°C. Intake oxygen concentration, O_{2in} , was maintained at 15 %, the coolant water temperature at 80°C and the swirl ratio at 1.6. The specifications of the nozzles used in the two chambers and the first and second fuel injections quantities and timings are also contained in the Table.

Figures 35 and 36 show the computational mesh respectively of the Stepped-lip re-entrant and of the new Divided combustion chamber. The simulation on the Stepped-lip chamber was conducted on a 36° sector mesh. In fact, being the in-cylinder gas behaviour axisymmetric, this was an useful method to decrease the calculation time. On the other hand, a full sector was adopted in the case of the Divided combustion chamber’s simulation, because the in-cylinder gas condition was strongly non-axisymmetric. The required calculation time increased greatly in this latter case. The average cell size was 0.5 mm and the total number of cells was around 1729000. The sub-models adopted in these cases were the same as the ones set in PART 1 and are summarized in Table 6.

Particular focus was given to the gasses temperature and to the O_2 mol concentration on a section across the combustion chamber as key factors to understand the air utilization status.

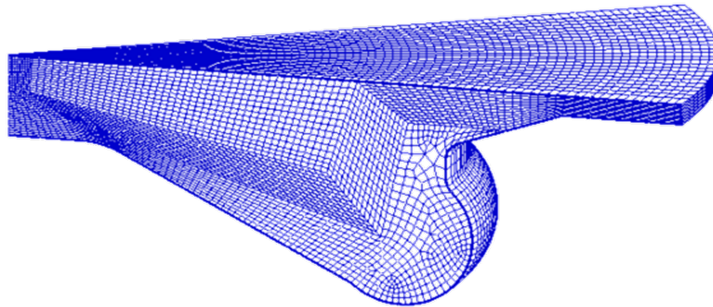


Figure 35: *Computational mesh of the Stepped-lip re-entrant combustion chamber*

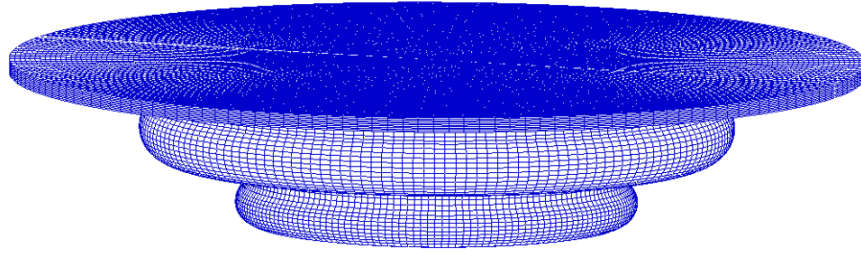


Figure 36: *Computational mesh of the new Divided combustion chamber*

5.3 Results and discussion

As it is possible to see in Figure 37, the results in terms of rate of heat release of the computational simulation and of the real-engine experiment on the Stepped-lip re-entrant chamber seem consistent. Also, regardless of the injector system, there is no significant difference in the combustion phase: it occurs almost over the same crank angles. In the case of the first injection, the heat release pattern is basically coincident, but in the case of the second, the heat release pattern is higher in the case of the two-injector system, suggesting that in that case fresh air entrainment is promoted.

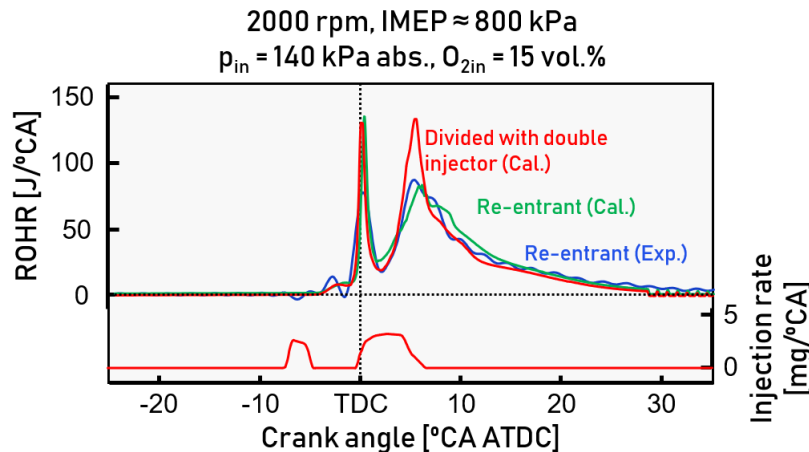


Figure 37: *Rate of heat release in new Divided and Stepped-lip re-entrant combustion chamber*

Figure 38 shows the variation of temperature and of O_2 concentration of in-cylinder gases on a section of the combustion chambers over the crank angle period from 2 to 8 °CA ATDC. This

interval is the one that goes from the end of the first fuel injection to the diffusive combustion of the second spray.

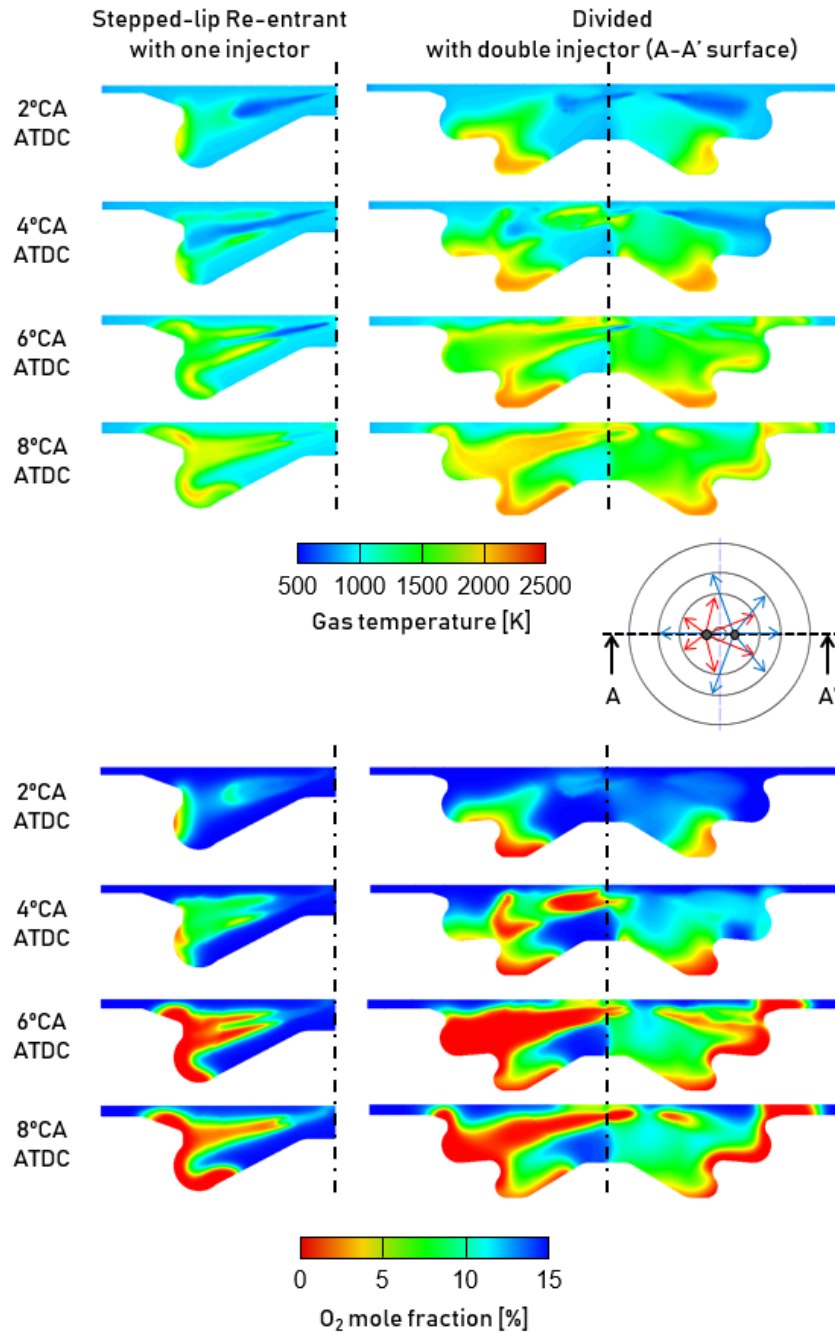


Figure 38: Temperature and O_2 distributions of in-cylinder gasses over the crank angle period from 2 to 8 °CA ATDC.

From the figure, it is clear the mechanism with which, in the case of the Stepped-lip re-entrant chamber, the second fuel spray enters the region of high temperature and low O_2 mole fraction region produced by the first injection's combustion.

In the case of the Divided combustion chamber, at 2°CA ATDC it is possible to see how the first fuel injection, burning, produces high temperature gasses and causes low O_2 concentrations mostly in the lower part of the combustion chamber. Moreover, it is possible to notice the asymmetry in the temperature and O_2 mole fraction distribution, due to the non-centred location of the injectors. At 2 °CA ATDC, in the left side of the Divided chamber, the high temperature burning gasses partially invade the upper part of the combustion chamber. At 4 °CA ATDC the second fuel injection in both chambers is starting to burn: in the left section of the Divided chamber this happens at a higher pace while proceeding more slowly in the right side. At 6 °CA ATDC the diffusion flame established in both chambers produces very low O_2 concentrations in the left area of the Divided chamber, while higher concentrations are maintained in the right part. Intermediate ratios are visible in the Stepped-lip re-entrant chamber. With reference to this latter one, it is possible to notice a wide portion of gasses containing 15 % O_2 , which indicates that still much air has not been mixed and has not been burned at this time.

The greatest area of improvement in the Divided chamber is found to be the right section, where a good separation of the fuel sprays and a better air utilization (lower final O_2 concentrations) seems to have been achieved.

It must be noticed that the asymmetry of the injection system causes an asymmetrical behaviour of the in-cylinder burning gasses. This makes it difficult to have a clear sense of the overall combustion performance.

Finally, from these simulations it is possible to say that the spatial separation with enhanced air utilization could be established when the two-stage heat release partially premixed combustion was performed with the new Divided combustion chamber and injection system. Further investigation and real-engine tests should be performed in the future research in order to analyse the real-engine performances under such conditions.

6 Conclusions

Partially premixed combustion, namely a combustion strategy which can be implemented in internal combustion compression-ignition engines, has been studied both on a real engine and through 3D CFD simulations. The initial input were the climate sustainability and the improvement of air quality which have been tackled by many researches in the past years through the continuous effort of improving the performance of such a large-scale spread transportation technology.

The work carried out by the previous researches has been analysed and among the numerous possible combustion strategies, partially premixed one was chosen for this project: a twin peak combustion involving a premixed flame followed by a diffusive flame. Primary goal was set as the improvement of the thermal efficiency along with the reduction of two of the engine-out air pollutants: NO_x and PM .

Firstly, a comparison of partially premixed combustion with conventional diesel combustion was carried out. A test bench was available, equipped with a single cylinder engine, a supercharger and a low pressure cooled EGR group. Conventional combustion strategy settings were chosen according to the Japanese Strategic Innovation Promotion Program, while partially premixed strategy's ones were tuned on the best results in terms of thermal efficiency of previous trials.

Under low and medium load conditions, the thermal efficiency showed an improvement for the non-conventional strategy, as a sum of the reduction of exhaust loss, increase of degree of constant volume and constant cooling loss. On the other hand, the increase of cooling loss prevented a similar improvement at high load conditions.

The main issue related to the premixed combustion was minimized thanks to the two split injections. In fact, the combustion noise, calculated from in-cylinder pressure data, increased, but the gap with conventional diesel combustion did not exceed 1.8 dBA at low load condition and 1 dBA at medium and high loads.

Moreover, at low and medium load conditions, the particulate level of both combustion

strategies was almost equivalent. NO_x levels increased in the partially premixed case and needed to be reduced by means of EGR. However, this could be successfully implemented without causing the deterioration of the soot levels. At high loads, partially premixed combustion produced lower levels of soot, but much greater NO_x quantities. Even if the implementation of EGR could lower the NO_x level, this caused an increase in soot which, differently from the previous cases, exceeded the conventional combustion soot levels.

In regards of the study of the combustion phase, achieved by varying the fuel injection timings, it was possible to notice that the thermal efficiency remained always higher for partially premixed combustion at any combustion phase (when the combustion phase was the same). This applied to low and medium loads, while for high loads the gap was almost negligible.

The second main topic of the study was the analysis of the behaviour of the in-cylinder gas mixture, by means of a 3D CFD software, AVL FIRE, with the implementation of a new designed combustion chamber and a double injection system. This whole arrangement was realised with the goal of promoting a better in-cylinder air utilization through a spatial separation of the first and second combustion events of the partially premixed strategy. To this end, the new combustion chamber was designed with a lip dividing an upper and a lower area. Two injectors were conceived together with two different cone angles: the “left” injector with a narrow angle and whose fuel sprays would aim at the lower part of the combustion chamber and the “right” injector, with a wider cone angle and whose sprays would aim at the upper section. Ultimately, the injection timings were set in a way that the burning spray entering the upper chamber would not invade the so-called squish area.

CFD results demonstrated that, with this system, it was possible to suppress, at least locally, the second fuel spray from entering the high-temperature, low-oxygen region left by the previous flame. Whereas, the same result could not be achieved when employing the conventional Re-entrant combustion chamber, and the second spray entering the burned gas left by the first combustion inevitably caused soot formation.

To sum up, this study points out the problem that with partially premixed combustion no remarkable improvement can be achieved at high load condition, but only at low and medium

loads. However, partially premixed combustion has high potential for high thermal efficiency and low NO_x and PM emissions.

In conclusion, further investigation on the possible benefits of partially premixed combustion implemented on the divided combustion chamber with a double injection system should be carried out by real-engine experiments, with the purpose of clarifying the outputs in terms of thermal efficiency, air utilization and emissions, especially at the most critical high load condition.

References

- [1] IPCC, 2014: Climate Change 2014: Synthesis Report. Contribution of Working Groups I, II and III to the Fifth Assessment Report of the Intergovernmental Panel on Climate Change [Core Writing Team, R.K. Pachauri and L.A. Meyer (eds.)]. IPCC, Geneva, Switzerland, 151 pp.
- [2] World Health Organization. Ambient air pollution: a global assessment of exposure and burden of disease. 2016.
- [3] Paris Agreement, United Nations 2015.
- [4] European Court of Auditors. The EUs response to the “dieseldate” scandal. European Union 2019.
- [5] Hiroyasu, Hosho, Oyama. Internal Combustion Engine, ISBN: 978-4-339-04067-8 .
- [6] JSAE Journal, paper No. 13.
- [7] European Environment Agency. Electric vehicles from life cycle and circular economy perspectives; TERM 2018: Transport and Environment Reporting Mechanism (TERM) report. EEA Report No 13/2018; 2018; ISBN 978-92-9213-985-8.
- [8] European Union. European Union emission regulations for new light duty vehicles—including passenger cars and light commercial vehicles;
<https://www.dieselnet.com/standards/eu/ld.php> .
- [9] European Environment Agency. Monitoring CO_2 emissions from new passenger cars and vans in 2017. EEA Report No 15/2018; 2016; ISBN 978-92-9480-002-2.
- [10] Heywood J B. Internal Combustion Engine Fundamentals, Second Edition. McGraw-Hill Education 1988; ISBN: 978-1-260-11610-6.
- [11] Kosaka H, Aizawa T, Kamimoto T. Two-dimensional imaging of ignition and soot formation processes in a diesel flame. SAGE; 2005.

- [12] World Health Organization. Evolution of WHO air quality guidelines: past, present and future. Copenhagen: WHO Regional Office for Europe; 2017; ISBN 9789289052306.
- [13] European Environment Agency. Emissions of the main air pollutants by sector group in the EEA-33; 2018;
https://www.eea.europa.eu/data-and-maps/daviz/share-of-eea-33-emissions-4#tab-chart_1.
- [14] Turns S R. An introduction to combustion, McGraw-Hill Education 2011; ISBN: 978-0-073-38019-3.
- [15] d'Ambrosio S, Ferrari A. Potential of double pilot injection strategies optimized with the design of experiments procedure to improve diesel engine emissions and performance. Appl Energy 2015; 155 : 918 - 932.
- [16] d'Ambrosio S, Ferrari A. Potential of multiple injection strategies implementing the after shot and optimized with the design of experiments procedure to improve diesel engine emissions and performance. Appl Energy 2015; 155 : 933 - 946.
- [17] Wagner U, Wiemer S, Velji A, Spicher U. An experimental study to assess the potential of homogeneous charge compression ignition diesel combustion with various fuels for light-duty engines. Institute for Reciprocating Engines, Universität Karlsruhe (TH) 2006.
- [18] Shimazaki N, Minato A, Nishimura T. Premixed diesel combustion using direct injection near top dead centre. Isuzu Advanced Engineering Center Limited 2007.
- [19] Akihama K, Takatori Y, Inagaki K, Sasaki S, Dean A M. Mechanism of the Smokeless Tich Diesel Combustion by Reducing Temperature. Society of Automotive Engineers 2001.
- [20] Mendez S, Thirouard B. Using Multiple Injection Strategies in Diesel Combustion: Potential to Improve Emissions, Noise and Fuel Economy Trade-Off in Low CR Engines. SAE International 2008.

- [21] Ogawa H, Li T, Miyamoto N. Characteristics of low temperature and low oxygen diesel combustion with ultra-high exhaust gas recirculation. SAE International 2016.
- [22] Ogawa H, Shibata G, Sakane Y, Arisawa T et al. Semi-Premixed Diesel Combustion with Twin Peak Shaped Heat Release Using Two-Stage Fuel Injection. SAE Technical Paper 2016-01-0741, 2016, doi:10.4271/2016-01-0741.
- [23] Japanese Strategic Innovation Promotion Program : <http://www.nagai.iis.u-tokyo.ac.jp/sip/aboutus/sip.htm>.